AD NUMBER
AD452957

NEW LIMITATION CHANGE

TO

Approved for public release, distribution unlimited

FROM

Distribution authorized to U.S. Gov't. agencies and their contractors; Administrative/Operational Use; Sep 1963. Other requests shall be referred to Naval Research Lab., Washington, DC 20375.

AUTHORITY

Naval Research Labs ltr dtd 27 Mar 1968

UNCLASSIFIED

AD. 4 5 2 9 5 7

DEFENSE DOCUMENTATION CENTER

FOR

SCIENTIFIC AND TECHNICAL INFORMATION

CAMERON STATION ALEXANDRIA, VIRGINIA

METALLURGICAL CHARACTERISTICS
OF
HIGH STRENGTH STRUCTURAL MATERIALS

P.P. Puzak, K.B. Lloyd, E.A. Lange,
R.J. Goode, and R.W. Huber

METALLURGY DIVISION

September 1963

CONTENTS

ABSTRACT

Explosion tear and drop-weight tear tests were con-
ducted on specially processed quenched and tempered
steels, on some maraging steels, and on some titanium
alloys. The fracture toughness relationships are
presented for these materials. The effects of pre-
cracking Charpy specimens of titanium on the shape of
the Charpy curve and on crack initiation in the Charpy
specimens are described. Preliminary crack growth
rate studies on an HY-80 steel, a Ti-6Al-4V alloy, and
a 2024 aluminum alloy, that were undergoing low-cycle
fatigue, are described. Alloy development and welding
studies on titanium are described and the mechanical
properties of an NRL as-cast Ti-7Al-2Cb-1Ta plate are
compared to those of a commercially produced plate of
the same alloy.

PROBLEM STATUS

This is a progress report; work is continuing.

AUTHORIZATION

ii

METALLURGICAL CHARACTERISTICS
OF
HIGH STRENGTH STRUCTURAL MATERIALS

INTRODUCTION

This is the second status report covering the Naval Research Laboratory's long-range program of determining the performance characteristics of high strength materials. Presently under investigation are maraging steels, quenched and tempered (Q&T) steels, titanium alloys, and aluminum alloys.

Explosion tear and drop-weight tear test (DWTT) results on some specially processed Q&T steels and maraging steels are covered in this report. The correlations between the fracture toughness, yield strength, and processing are developed for both of these steels using fracture analysis diagram procedures. The growth rate of cracks in a representative alloy of steel, of titanium, and of aluminum has been studied and a preliminary relationship between crack growth rate and strain range for the materials is presented. Charpy V-notch, drop-weight tear, and explosion tear tests have been conducted on a number of titanium alloys. The results of these studies are presented along with a preliminary generalized description of the relationships between the various fracture toughness tests on titanium.

Also included is a study of the effects of pre-cracked Charpy specimens on the shape of the Charpy curve and on crack initiation for titanium alloys. The results of welding studies on several titanium alloys are discussed, including the fracture toughness properties of the welds. The mechanical and fracture toughness properties of an NRL as-cast Ti-7Al-2Cb-1Ta plate are reported and these properties are discussed relative to commercially produced material.

1

INVESTIGATION OF FRACTURE TOUGHNESS OF HIGH STRENGTH STEELS CONSIDERED FOR DEEP SUBMERGENCE SUBMARINE HULLS
(P.P. Puzak and K.B. Lloyd)

Because long-time welding fabrication experience has demonstrated that "flaw-free" construction cannot be assured, or maintained in service applications involving cyclic stresses, service reliability of large, heavy-section structures is dependent upon type of performance in the presence of flaws. For any given material at a given temperature, it is now known that the size and acuity of a flaw determines the stress level required to initiate catastrophic fracture. Thus, to provide fracture-safe structural reliability, flaw size, stress level, and temperature requirements for fracture must be known, or developed, for the materials considered for use. Reliable procedures have been evolved for evaluating these relationships for the low-hardness, structural steels that are characterized by low (100 ksi or less) yield strengths. These procedures are based on the concept of the fracture-analysis diagram which depicts the relative stress levels for a spectrum of flaw sizes required for fracture at temperatures above, or below, the nil-ductility transition (NDT) temperature of the material involved. A comprehensive description of the development of this new concept, with detailed service failure data provided as documentation of its validity, for the fracture-safe engineering use of the low-strength steels has been reported (1).

Although there is a wealth of data for high strength sheet metal, this data cannot be extrapolated to establish significant criteria for performance of heavy-section materials; and, there are not much valuable fracture stress data available for the latter. One phase of NRL studies is aimed at developing information regarding catastrophic fracture in high strength materials in a manner similar to that now given for the low strength steels by the fracture analysis diagram procedures.

DEVELOPMENT OF FLAW SIZE-STRESS LEVEL REQUIREMENTS FOR FRACTURE IN ULTRAHIGH STRENGTH HEAVY-SECTION STEELS

The explosion tear test (ETT) and drop-weight tear test (DWTT) are new methods devised for full-thickness test evaluations of fracture toughness in high strength materials at any test temperature. Because the findings

with these methods are aimed at establishing the potentials
of high strength materials for submarine hull applications,
these tests have been conducted primarily at the lowest
service temperature of interest, viz., 30°F. The ETT
method features sharp, weld-crack flaws which are developed
in large plate specimens by special "patch" welding
techniques. By varying the flaw size and explosive loading
intensity, this method provides for investigations of flaw
size-fracture stress effects with a given material, or the
method can be used to compare the performance of different
materials in the presence of similar-size flaws. All ET
tests conducted to date have employed a flaw of 2-in.
length.

The DWTT features a composite weldment of a smaller plate
section of the high strength "test" material joined to a
notched, brittle, cast-steel bar. These specimens are
loaded as beams by the action of a falling weight in order
to determine the specific energy absorption levels which
result in continued propagation of the brittle, "traveling"
crack for unit distances in the "test" material. Correla-
tions of results obtained by both methods for numerous
steels have shown that fracture toughness of a given steel,
as demonstrated in the precracked ETT, is directly relat-
able to the energy absorption values measured for the same
steel in the DWTT.

EXPLOSION TEAR AND DROP-WEIGHT TEAR TESTS OF QUENCHED AND
TEMPERED STEELS

The general relationships which exist between DWTT energy
values and ETT performance for Q&T steels were established
by the earlier studies (2). These studies involved a
variety of Q&T steels and one maraging steel*, which were
DWT tested in both orientations while the ET tests were
conducted with fracture propagation only in the "weak"
direction of the plates. The steels with DWT energies of

---

* Approximately 230 ksi yield strength maraging steel of
the 18% Ni - 7-1/2% Co - 5% Mo type.

3

3000 ft-lbs or more ("weak" direction) exhibited high
fracture toughness as indicated by the development of
limited tears in the 2-in. flaw ETT specimens subjected
to relatively high (5 to 7%) plastic deformation loads.
More extensive tearing was observed in the steels with
DWT energies which ranged from 2500 to 1000 ft-lbs. The
maraging steel which was characterized by 500 ft-lbs DWT
energy broke "flat" in the ETT conducted with an elastic
stress level load.

The ETT samples shown in Fig. 1 illustrate the previously
documented extremes in performance of steels tested in the
presence of a 2-in. crack. It is obvious that the frac-
ture stress for a 2-in. flaw in the maraging steel shown
at the left is at elastic levels of load - the plate
remained perfectly flat. The high fracture toughness
level in the "weak" direction of a poorly cross-rolled
HY-80 plate shown at the right is documented by the ob-
served propagation of short, limited tears for each of
five successive plastic level load applications. In
other words, even with the enlargement of the original
2-in. flaw to almost 1-ft length and loading which ap-
proached the ultimate tensile strength of the steel (deep
bulge), fracture propagation was resisted by the HY-80
steel. Complete 45-degree shear fractures of DWTT speci-
mens of this HY-80 steel were obtained with 3500 ft-lbs
in the "weak" direction and 7750 ft-lbs in the "strong"
direction.

A summary of the relationships between DWTT energy values
and strength level for all Q&T steels tested to date is
given in Fig. 2. The lower curve shows the limit of
fracture toughness developed for conventionally rolled
and processed steels when tested in the "weak" direction;
the upper curve, the limit developed with steels of
special melting and processing practices. The DWTT
energy values for the conventionally rolled and pro-
cessed steels tested in the "strong" direction are not
shown in Fig. 2. However, the "strong" direction values
for the conventionally rolled and processed steels at any
given strength level were found to reside above the "weak"
direction limit curve and below the data points for the
special melt practice steels. The maximum strength level
Q&T steel tested to date is noted to be approximately
180 ksi yield strength (YS). The dashed portions of the

4

curves in Fig. 2 were based upon the previously described
results obtained with the one 230 ksi YS maraging steel.
The plotted DWTT values represent the energies for complete
fracture of the standard specimen obtained by "bracketing"
within an increment of 250 ft-lb tests of several specimens.
As noted in Fig. 2, tests are not conducted with less than
500 ft-lbs because an energy of at least 400 ft-lbs is re-
quired to develop the crack in the brittle casting portion
of the DWTT specimens.

It is also demonstrated in Fig. 2 that different composi-
tion steels of a given strength level varied widely in
tearing resistance. In reheat treatment studies conducted
with these steels, all exhibited decreasing levels of frac-
ture toughness with increasing strength levels. Another
important finding is that the tearing energy of a given
steel was found to vary widely with specimen orientation.
Thus, as indicated by the curves in Fig. 2, the practicable
upper limit of fracture toughness for any given strength
level is a function not only of composition and heat treat-
ment, but also of mill-processing variables (cross-rolling
and melting practices).

The Q&T steels exhibit transition temperature features
such that the fracture mode changes from shear to cleavage
with decreasing temperature. The present stage of cor-
relation development precludes the use of Charpy V (C_v)
specimens for evaluating toughness of Q&T steels at tem-
peratures which entail a mixture of fracture modes.
However, the correlation of DWTT energy values with C_v
shelf energy (full shear fractures at 30°F) values is
surprisingly good; all of these relationships established
for Q&T steels to date are shown in Fig. 3. The dashed
curves in Fig. 3 represent the data band which encompassed
these relationships established in the earlier studies for
Q&T steels. As noted in Fig. 3, only three of the Q&T
steel data points included in this illustration fall out-
side the previously established correlation band for DWTT
energy values with C_v shelf energy values.

Nine of the recently tested Q&T steels represent material
from a single electric furnace heat conforming to the
chemical composition requirements of "high-chemistry"
HY-80, Table I. These steel plates were specially
processed to obtain various degrees of production "cross-
rolling" and three levels of YS by Q&T heat treatments with

5

tempering temperatures of 1050°, 1100°, and 1150°F.
Tension, C_v, and DWT tests on these steels were conducted
in both orientations. The data are given in Table II.
ET tests were conducted with fracture propagation only
in the "weak" direction. The significance of the DWTT
energy value to ETT performance can be illustrated by
the results obtained for the nine specially rolled
HY-80 steels described above. The data given in Fig. 2
are replotted in Fig. 4 to highlight the relative
position and values obtained for these specially proc-
essed steels, numbers 1 to 9 in the illustration.
ET tests of these steels were conducted with a 2-in.
flaw and loading conditions of 5 to 7% strain. As in-
dicated by the arrows and data shown in the lower right
portion of Fig. 4, significantly longer crack lengths
are developed by the ETT specimens with decreasing DWTT
values from 2250 to 1000 ft-lbs. The corresponding de-
crease in C_v energy values for these steels ranged from
approximately 40 to 23 ft-lbs. The ETT samples of these,
Fig. 5, illustrate the dramatic change in toughness
developed by the Q&T steels with DWT energies increasing
from 1000 to 2250 ft-lbs (compare performance of steel
No. 1 to that illustrated for steel No. 9).

EXPLOSION TEAR AND DROP-WEIGHT TEAR TESTS OF MARAGING
STEELS

The maraging materials comprise a considerable variety
of virtually carbon-free steel compositions which may be
heat-treated to high strength levels by aging at tempera-
tures up to 1000°F. The strength levels attained as a
consequence of the precipitation and ordering processes
which occur on aging depend upon the composition, aging
time, and aging temperature. Most of the available in-
formation concerning the properties of the maraging
steels have been developed with material from relatively
small (30 to 100 lbs) laboratory melts. Although some
large tonnage, production heats of maraging steels have
been produced, these have invariably been limited to those
compositions capable of developing YS in the range of 250
to 300 ksi when aged at 900°F (3). Analyses of the
available data indicates that the toughness properties
are generally lower for production material than that
measured for the small, laboratory melt material.

In addition to the one previously tested maraging steel, fracture toughness evaluations of eleven experimental maraging steels have been completed. The 1-in. plates obtained for these studies were rolled from 1-ton and 1/2-ton heats of the maraging steel compositions given in Table III. The melting practice for these steels generally involved consumable electrode-vacuum melting (CEVM), however, air-melted heats of the compositions recommended for 150 and 200 ksi YS were included. The maraging steels studied in this investigation (Table III) were all aged for 3 hours at 900°F, the treatment usually recommended to develop maximum YS. For some steels, annealing temperatures of 1700° and 1900°F were used because exploratory studies had indicated that slightly better C_V energy absorption values were developed by the materials after annealing at these temperatures than were possible when annealed at the customary 1500°F.

Tension, C_V, and DWT tests on the maraging steels were conducted in both orientations. The data are given in Table IV. ET tests were also conducted with fracture propagation only in the "weak" direction. The results indicate generally similar correlations between flaw size and stress-for-fracture as those established for Q&T steels. A summary of test results for the maraging steels is provided in Fig. 6. The curves for Q&T steels (from Fig. 2) have been included for purposes of comparison. The lines joining the symbols for "weak" and "strong" directions indicate results obtained for the same steel in the two orientations. From the small difference in DWT values with orientation (500 ft-lbs or less), it is apparent that the 1-in. plates produced from 1-ton heats had been highly cross-rolled, as indicated by the producers. The 1-in. plates produced from 1/2-ton heats, however, had been rolled with conventional practices, and the DWT energy values differed with orientation by approximately 1500 and 2000ft-lbs.

The ultrahigh strength maraging steels of the 18% Ni-Co-Mo type do not exhibit distinct transition temperature features, but are generally characterized by poorly defined, low-slope, C_V transition curves.

7

Electron fractographic studies of C_v specimens (conducted by Beachem and Dahlberg) have demonstrated that the fracture mode in these steels comprises a "dimple rupture" (characteristic of shear-mode fractures), even at the low temperature of liquid nitrogen. The maraging steels of 10 to 12% Ni-Cr-Mo type (YS of approximately 150 to 165 ksi) were found to develop significantly high C_v energy values at 30°F, ranging from approximately 50 to 100 ft-lbs. With decreasing temperatures, these steels exhibited typical transition curves showing decreasing C_v energy values. Preliminary electron fractographic studies have indicated that a change in fracture mode may be involved because "dimple rupture" was observed in the C_v specimens tested at 30°F, and areas of "quasi-cleavage" rupture in the C_v specimens tested at -200°F. Nevertheless, the correlation of DWTT energy values with C_v energy values at 30°F for all the maraging steels appears to be similar to that established for Q&T steels, as shown in Fig. 7. The dashed curves in this figure represent the data band which encompassed all DWT and C_v energy relationships established for Q&T steels (2).

Whether or not the C_v test will provide an acceptably accurate correlation between flaw size and stress-for-fracture in the 18% Ni maraging steels of 200 ksi YS and higher cannot be determined at this time. One anticipated difficulty is that the range of C_v energy values will be too narrow (15 to 20 ft-lb spread), as is suggested by the clustering of data points in the extreme lower left portion of the data band in Fig. 7. However, it is significant to note that the relationships of C_v energies with YS for maraging steels, Fig. 8, indicate similar findings as those described earlier for Q&T steels, viz., (1) different composition steels of a given strength level vary widely in tearing resistance, (2) decreasing fracture toughness levels with increasing strength levels, and (3) a practicable upper limit of toughness for any given strength level is a function of composition, heat treatment, and mill-processing variables (cross-rolling and melting practices).

The significance of DWTT energy values to ETT performance for the maraging steels is found to be remarkably similar to that established for Q&T steels. The data given in

8

Fig 6 are replotted in Fig. 9, in order to highlight the
values obtained for the steels, numbered 10 to 16 in the
illustration. The "weak" direction DWTT values for
these steels are noted to range from 5500 to 500 ft-lbs
and the C_v values at 30°F (arrow and data in Fig. 9 left)
range from 99 to 14 ft-lbs. Steel Nos. 10 and 11 devel-
oped more than 3000 ft-lb DWT energies. These steels
exhibited limited tearing in the 2-in. flaw, ET tests at
moderately high (5 to 7%) plastic strain levels of
loading by representative samples, Fig. 10, top. The
high toughness level indicated by these steels is
characteristic of the performance developed by the Q&T
steels of more than 3000 ft-lb DWT energies. Similar
loading conditions used on steel Nos. 12 and 13 (approx-
imately 200 ksi YS) resulted in the development of com-
plete fractures, Fig. 10, bottom). The partial rupture
shown by steel No. 12 resulted from the presence of a
large lamination in this plate.

Steel No. 14 represents material from the 10-ton air-
melt heat which was shown, Fig. 1, to break "flat".
The ETT conditions employed for steel Nos. 15 and 16
also involved elastic stress levels. The performance
of steel No. 15 in the presence of a 2-in. crack is
illustrated by Fig. 11, left. One-half of the plate
remained perfectly flat, indicating that the fracture
propagated at elastic levels of load; the other half
was pushed out upon contact with the die after the
complete fracture was developed. Complete fractures
of DWTT specimens of this steel were obtained with 750
ft-lbs. The same elastic level loading conditions were
used for ET tests of steel No. 16. Here, in addition
to "flat break" performance in the presence of a 2-in.
crack, extensive fragmentation was developed, as shown
in Fig. 11, right. Complete fractures of DWTT specimens
of this steel were obtained with 500 ft-lbs.

LOW-CYCLE FATIGUE AND CRACK GROWTH RATES IN HY-80, Ti-6Al-4V AND 2024 ALUMINUM
(E.A. Lange)

As the trend for increased performance from structures
continues, the requirement for good low-cycle fatigue
characteristics increases. This is partially due to

increased nominal elastic strain resulting from the high loads which also cause increased plastic strain at regions of strain concentration from either design features or flaws. Low-cycle fatigue properties include an evaluation of the resistance to the initiation of fatigue cracks at regions of strain concentration and an evaluation of the resistance to the growth of fabrication flaws already in the material. The answer to the question of whether the crack initiation or the crack propagation characteristics control the working life of a structure, depends upon the design of the structure and the quality of the fabrication. Separate evaluation of the factors involved in the two characteristics must be made. It is the aim of this study to determine the growth rate of fatigue cracks in all high strength materials, and these initial results were obtained with a representative alloy of steel, of titanium, and of aluminum.

It is emphasized that the relationships developed from these preliminary data are tentative and they are presented at this time to indicate trends rather than to act as a direct comparison of the three materials.

EXPERIMENTAL PROCEDURE

A detailed description of the experimental procedure was presented in the First Quarterly Report, Ref. 4. Briefly, a bar-shaped specimen which has a test section 0.5-in. thick and 2.5-in. wide is loaded as a cantilever beam in a hydraulic machine at a rate of 5 cycles per minute. The specimen is the Lehigh design, and the machine was developed by the U. S. Navy Marine Engineering Laboratory. Since the test concerns the growth of fatigue cracks, the initiation of the crack is enhanced by a 1/4-in. long mechanical notch in the center of the reduced section. The length of the crack is measured with an optical micrometer, and sufficient measurements are made to continually monitor the growth rate of the crack. Because the increase in the length of the crack may be less than 0.0001-in. per cycle, the strain range is held constant for periods extending from 1000 to 3000 cycles until the crack growth rate is established, and then a different strain range is used for another

short period of cycles. With this procedure the crack
growth rate can be determined for various ranges of
strain and crack lengths using a single specimen. Data
from specimens in the three materials considered in
this report are listed in Table V. It is hoped that
reduction of the data from this approach will reveal
an interrelationship between crack growth rate, strain
range, and crack length. For orientation purposes the
tensile properties of the three materials of concern in
this report are listed in Table VI and compared in
Fig. 12.

Although the nominal stresses in structural members
from all probable loads are in the elastic range,
i.e., below YS, excessive strains may occur at geo-
metric features which interrupt the uniform distribu-
tion of strain. Localized plastic strain occurs
frequently at design features such as at changes in
thickness or junctions of members and at unintentional
flaws such as welding cracks or material imperfections.
The localized plastic strain fields at the tips of
cracks are shown schematically in Fig. 12. These
localized regions of strain concentration can cause
fatigue cracks to grow to a critical size in less than
100,000 applications of load, and thus failure can
occur in the low-cycle range of fatigue.

Since an analysis of these strain zones for various
materials and stress fields is not possible, the
effect of these strain zones on the growth rate of
fatigue cracks is determined in terms of the nominal
strains which surround the zones and can be measured.

During a test the nominal strain range in the specimen
is controlled by controlling the deflection of the
specimen. The strain range, tension strain plus com-
pression strain, is used in the reduction of the data,
because this is the strain wich is indicated by a
strain gage in a critical region of a working structure
where the position of zero strain is not known due to
the deformation which occurs during fabrication and
shakedown. The elastic strain in a test specimen of
any material is a function of specimen geometry and is
dependent upon the deflection of the specimen. However,
the deflection that initiates plastic strain is not the

11

same for each material and varies with the elastic modulus and the proportional limit. This can be seen when the strain-deflection relationships of the Lehigh specimen for the three alloys in this study are compared in Fig. 13. Since the nominal strains involved in low-cycle fatigue generally range from one-half of the strain at the proportional limit to strains including 0.1% plastic strain, it is readily apparent that for cyclic load conditions, the 0.2% plastic strain considered to be relatively small in a tensile test is a very large plastic strain for fatigue. The insidious nature of low-cycle fatigue failures results from the growth of cracks from very small plastic strains around obscure structural defects.

CRACK LENGTH FACTOR

In attempting to reduce the crack growth rate data for the three materials on a common basis, it became apparent that the complex, two variable factor proposed in Ref. 4, $\epsilon_t \sqrt{CL}$, did not correlate with the crack growth rates observed for the titanium alloy and the aluminum alloy as well as it did for steel. This was due primarily to the greater sensitivity of these alloys to changes in strain range, and the use of the complex factor emphasized excessively the importance of crack length. In order to determine a more appropriate evaluation of the effect of crack length on crack growth rate, all of the data for HY-80 steel obtained at the strain range of 6730 μ in./in. were graphed, Fig. 14, to obtain the best exponential value for this factor from this preliminary data. A slope of 2/3 is obtained on a log-log plot. Due to the lack of more extensive data, this exponent was then assumed for the crack length variable for all of the materials. When the equation expressed crack growth rates in terms of unit crack length, a more appropriate evaluation of strain range was obtained; thus:

$$CR/(CL)^{\frac{2}{3}} = k\,\epsilon_t$$

where: CR = Crack growth rate; CL = Crack length;

ϵ_t = Strain range; and   k = Constant

STRAIN RANGE FACTOR

The effect of strain range on the growth rate of low-cycle fatigue cracks in HY-80, Ti-6Al-4V, and 2024 aluminum from these preliminary data is shown in Fig. 15. A trend for increased sensitivity to strain range in the order of HY-80 : Ti-6Al-4V : 2024 Aluminum is indicated by the slopes of the lines. Because of the variation in the tensile properties of these alloys, comparisons of crack growth rate characteristics must be made on more than one basis to present a more complete picture. Table VII compares the crack growth characteristics of the three alloys on the following basis: (a) the sensitivity to strain range as the exponent in the equation $CR/(CL)^5 = \epsilon^m$, (b) crack growth rate for a strain range in the elastic range which would be the case for a specific structural configuration and load, and (c) crack growth rate for a strain range essentially at the proportional limit, 0.01% plastic strain.

For these three initial materials tested, the resistance to the growth of fatigue cracks is highest in HY-80 steel on the basis of these three comparisons. Although the relationships in Fig. 15 are tentative, they illustrate the effectiveness of the experimental procedure for evaluating the crack growth characteristics of a wide variety of material.

Proceeding studies are scheduled to improve and extend this method of low-cycle fatigue testing with a wide variety of alloys in the various base metals, especially the new high strength materials, and also to evaluate the effects of directionality due to processing conditions.

MECHANICAL PROPERTIES OF TITANIUM ALLOYS
(R.J. Goode and R.W. Huber)

Tensile and fracture toughness properties were determined for some high and low interstitial titanium alloys in the as-rolled and heat-treated condition. The Charpy and tensile specimens were obtained from expended DWTT specimens. Some of the tensile and fracture toughness data

presented in the First Quarterly Report (4) is presented
here for comparison purposes. ETT has been initiated on
these materials. The results of these studies to date
are presented in a series of generalized curves of Charpy
V-notch and DWTT energy with YS and temperature. Briefly,
the fracture toughness decreases with decreasing tempera-
ture and increases with YS and interstitial content. The
relationships between the DWTT and the Charpy V-notch
test is similar to that of steels.

TENSILE PROPERTIES

The room temperature tensile properties of all the
materials covered in this report are presented in Table
VIII. The specimens were tested in a Baldwin tensile
testing machine at a strain rate of 0.002 in./in./min.
The yield strengths were determined using the standard
0.2% offset on the stress-strain curve. Two specimens
of each orientation were tested, except for plate T-26
in which two specimens of one orientation were tested,
and the results averaged. When a significant variation
with orientation was encountered in any of the materials,
the average values for each direction are given. Other-
wise the maximum variations of the YS and UTS (ultimate
tensile strength) values, due to the directionality of
the plates, are less than ± 2% of the values given. The
maximum variation of the % RA and % Elong. are with ± 5%
of the values given.

Plates T-7 (Ti-5Al-2.5Sn), T-8 (Ti-6Al-4V), and T-9
(Ti-13V-11Cr-3Al) were obtained from the DOD Sheet
Rolling Program and are high interstitial materials.
They were tested only in the as-rolled condition since
DWT tests indicated no improvement in fracture toughness
after heat-treatment. The other materials are all of low
interstitial content (see Tables II and III in Ref. 4 for
latest chemical analysis of these materials). The tensile
properties of these alloys in the as-rolled condition are
presented, along with the properties after heat treatment,
for comparison purposes. The tensile specimens of the low
interstitial alloys that were heat-treated in vacuum (VAC)
for one hour were obtained from the as-rolled DWTT speci-
mens and then heat-treated. Those that show a two-hour

14

heat-treatment followed by an air cool (AC) were obtained from the heat-treated DWTT specimens. The tensile properties of the NRL as-cast Ti-7Al-2Cb-1Ta plate T-26 and the as-received hot-rolled and annealed Ti-7Al-2Cb-1Ta plate T-33 are also included.

FRACTURE TOUGHNESS TESTS

A description of the DWTT and the specimen configuration has been given in Ref. 4. The DWTT energy absorption values of the titanium alloy plates in the as-rolled and heat-treated condition are shown in Table IX. The DWTT values for plates T-26 and T-33 are included. It was possible to test the high interstitial plates T-7, T-8, and T-9 in only the RW direction (Ref. 5). The data for these plates indicate the lowest energy level at which tested and that the specimens broke at that energy level. The low interstitial plates T-19, T-20, T-21 and T-22 were tested in both the RW and WR directions in a as-rolled condition, but only in the WR direction in the heat-treated condition. The increase in fracture toughness, as measured by the DWTT, by heat-treatments 50 to 60°F below the β transus for plates T-20, T-21, and T-22 is significant. Plate T-19 was heat-treated slightly above the β transus. The Charpy V-notch properties of these heat-treated DWTT specimens are shown in Fig. 16. The Charpy V-notch data for plate T-33 has not yet been obtained.

A high interstitial unalloyed titanium, plate T-17, similar to plate T-2, and an Ti-8Al-2Cb-1Ta, plate T-23, were tested in the ETT. A description of this test, including the specimen configuration, and the use of this test along with the DWTT (in fracture toughness assessments of high strength steel plate material) is described in Ref. 2.

Each ETT specimen contained a sharp, 2-in. weld crack which was developed by cyclic loading the brittle crack starting weld in a large hydraulic press. In the tests the specimen of plate T-17 was subjected to an explosive loading calculated not to exceed the YS of the material, i.e., 0% strain deformation, and the

specimen of plate T-23 was explosively loaded to 5-7% strain deformation. From the DWTT and Charpy data complete failure of the specimen at these strain deformation levels was expected if the criteria developed for steels also held for titanium. The stand-off distance of the explosive necessary to produce the prescribed amount of strain deformation charge was determined for each alloy using the YS and plate thickness relationships developed for steels. The YS, Charpy, and DWTT data used in determining the test conditions for these two alloys are shown in Table X. The specimens were tested in the WR orientation, and the results of the tests are shown in Figs. 17 and 18.

The results of the explosion tear tests indicate that the notch fracture toughness criteria developed for steels may apply to titanium as well. A number of alloys covering a wide spectrum of strengths and DWTT energies are scheduled to be explosion tear tested to determine the exact DWTT and ETT relationships.

The results of these notch fracture toughness studies obtained to date are shown in a series of generalized curves, Fig. 19 through Fig. 22. Of course, these relationships are subject to modification or change as more materials are tested and more data becomes available. The relation of Charpy V-notch properties of titanium alloys in different ranges of yield strengths with temperature is shown in Fig. 19. The Charpy V-notch energy decreases with decreasing temperature and increasing YS. These energies are represented by bands at different YS levels. Within these bands there is some overlapping of yield strengths, i.e., in the 110-115 ksi band a 105 YS alloy may show lower C_v energy values than a 110 alloy, but generally for each band the lower YS materials fall in the upper portion of the bands and the higher YS in the lower portions of the bands. The effects of oxygen on fracture toughness and YS on unalloyed titanium is also indicated. The 33 ksi YS material has .07% oxygen and the 83 ksi YS material has approximately .17%. Generally for the alloys the trade-off of C_v and YS is not as great as that indicated for unalloyed material.

The relationship between the DWTT and C_v energy values is shown in Fig. 20. Superimposed on this plot is the Charpy shelf vs. DWTT band for steels (Ref. 2). At DWTT energy above 2000 ft-lbs the C_v-DWTT relationship is essentially the same for titanium and steels. Below 2000 ft-lbs the points for titanium lie below the steel band. In this region it appears that the DWTT is more discriminatory between the titanium alloys than is the Charpy V-notch test. The relationship of fracture toughness, as measured by Charpy V-notch and DWT tests, with YS is shown in Figs. 21 and 22. For the two tests the relationship is the same - a general over-all decrease in fracture toughness with increasing YS. The maximum fracture toughness limit (MFTL) is shown in each figure. The MFTL represents the optimum in fracture toughness of all the titanium alloys studied at NRL to date. It demonstrates the potential level of fracture toughness that should be obtainable with alloys of different yield strengths if the best combinations of melting, processing, and heat-treatments are followed in conjunction with control of interstitial content. The MFTL may shift to higher fracture toughness with the development of new alloys or processing techniques.

CHARPY V-NOTCH TEST - STANDARD vs. PRE-CRACKED TITANIUM SPECIMENS

The amount of energy required to separately initiate a crack and then propagate it through the test areas of a Charpy V-notch specimen was studied in a number of titanium alloys using standard and pre-cracked Charpy V-notch specimens.

The cracks were introduced at the notches of the specimens to a depth of 1/64 in. to 3/64 in. with a ManLabs Fatigue Pre-Crack Machine. The standard and pre-cracked specimens were tested in the same manner and the values obtained with the pre-cracked specimens were corrected to correspond to the area tested in the standard specimens as follows:

$$C_v^1 = \frac{W}{\dfrac{A_f}{A}}$$

17

where:

$C_v{}^1$ = corrected pre-crack energy absorption value

W = energy absorption measured with pre-cracked specimen

A = test area of standard Charpy V-notch specimen

A_f= test area of pre-cracked Charpy V-notch specimen

The test results are shown in Figs. 23 through 28. The pre-cracked specimens show lower energy absorption values compared to the standard ones, as would be expected, and the curves for the two types of specimens generally parallel each other for the same alloys. Since the amount of energy required to start a sharp crack moving through the test area of a pre-cracked specimen is only a small fraction of the amount needed to initiate a crack in a standard specimen of the same material, this difference in energy absorption can be considered to represent the amount of energy necessary to initiate the crack at the root of the notch in a standard Charpy V-notch specimen.

The relationship of energy required for fracture initiation in the standard specimens with temperature for the different alloys is shown in Fig. 29. Here it is seen that the energy required to initiate a crack is different for the different alloys and that this energy is temperature dependent up to some critical temperature which is also different for the different alloys. Above this critical temperature the energy requirement remains constant or possibly decreases slightly for each alloy.

The results of this study on titanium alloys indicate that there is essentially nothing to be gained in using pre-cracked in lieu of standard specimens. Pre-cracking the specimens prior to testing results only in shifting the C_v curves to lower fracture toughness values, though not by large numerical amounts, with the curves for both type of specimens paralleling each other. It does not change the shape of the curve appreciably in

18

that a sharp change in fracture toughness with small
changes in temperature (fracture toughness transition)
does not develop for any of the alloys investigated.
This study is going to be extended to steels to deter-
mine what effects pre-cracking has on the fracture
toughness curves of these materials.

ALLOY DEVELOPMENT, WELDING AND CASTING OF TITANIUM ALLOYS
(R.W. Huber and R.J. Goode)

The properties of an extra-low interstitial as-cast
Ti-7Al-2Cb-1Ta plate having a large grain size was
studied. A high DWTT energy was obtained for this
plate indicating large grain size is not detrimental
to fracture toughness. The addition of small amounts
of yttrium to unalloyed titanium was found to drasti-
cally reduce the fracture toughness of the material.
Welding studies show that the fracture toughness
properties of weldments on some titanium alloys are
roughly equivalent to those of the base plates.

PROPERTIES OF CAST TITANIUM ALLOYS

Properties of selected cast titanium alloys are being
studied due to their importance per se and also be-
cause of their similarity to weld deposited metal.
The effect of medium to large grain size on the notch
fracture properties of a typical near alpha titanium
alloy was qualitatively determined, the purpose being
to compare a large as-cast grain structure (larger than
that produced by a 25,000 joules per inch MIG-type
weld) with the usual grain size of a hot-rolled,
processed plate.

For this purpose a titanium 7Al-2Cb-1Ta extra low
interstitial alloy (estimated O_2 <.04%, N_2 <.004%) was
double vacuum arc-melted and skull cast into a 4 in.
x 7 in. x 12 in. copper chill mold. The large equi-
axed alpha prime grain structure is shown in a macro
section through the billet in Fig. 30. Charpy V-notch
specimens were prepared of the as-cast alloy and the
test data is presented in Fig. 31. The alloy in this
form had an UTS of 97 ksi, .2% YS of 93 ksi, 9.3%
Elong. in 1.4-in. gage and 38% RA.

One-half of the cast billet was forged at 2000°F starting temperature into a 1-1/2 in. x 5 in. x 18 in. slab, then hot-rolled in the six inch two high laboratory rolling mill to a 1 in. x 5 in. x 29 in. plate section.

Standard DWTT specimens of the rolled plate and as-cast metal were prepared with brittle crack starter welds and tested at 32°F, giving tear energies of 3250+ and 3500+ ft-lbs respectively. These values at equivalent YS levels are comparable to the NRL titanium 8Al-2Cb-1Ta alloy in the β heat-treated condition. Of all the alloys tested to date only one other alloy, Ti-6Al-4Zr-1V, has shown a higher (3750 ft-lbs) tear energy. Another comparison can be made with a commercial wrought sample of E.L.I. 721 alloy plate submitted by the USN Applied Science Laboratory. This material indicated a DWTT energy of 2750 ft-lbs which may be high due to underbead cracking of the crack starter weld.

It must be concluded that a large grain size for this type of titanium alloy is not detrimental to the notch fracture toughness. However, the YS for this type of alloy is considerably below the 120 ksi level.

TITANIUM ALLOY DEVELOPMENT

The effects of small additions of yttrium upon the notch toughness of titanium were ascertained in a limited exploratory study. Small 200 gram button melts containing .65, 1.25, 2.5 and 5% Y were prepared in a non-consumable arc furnace. The buttons were hot forged to 1/2 in. bar for C_v specimens, and the limited test data presented as curves are shown in Fig. 32. Charpy values of 150 to 200 ft-lbs for the unalloyed base titanium are drastically reduced by small additions of yttrium. All of the fracture surfaces displayed a very fine fibrous structure due in part to the method of fabricating. However there appears to be a grain refining by the yttrium additions. Hardness measurements gave values equivalent to or slightly less than the base 80-BHN electrolytic titanium indicating a gettering action or scavenging of the residual interstitials. There is essentially no solid solution hardening of titanium alloyed with up to 5% yttrium.

20

Two 12-lb experimental titanium alloys in the 130 to 140 ksi YS level are in process. The first melt ingots after quartering longitudinally are now being re-melted.

A titanium-40 molybdenum 10-lb ingot has been vacuum arc-melted and the ingot machined into chips for use in master alloy additions. This allows for a more uniform distribution of small additions of Mo to other titanium alloys.

WELDING OF TITANIUM ALLOYS

MIG welding (referring to a consumable electrode wire metal, inert gas process) has been used for joining 1-in. titanium alloy plates. Low interstitial alloy wires of three compositions - 5Al-2.5Sn, 6Al-4V, and 8Al-2Cb-1Ta - have been used for joining plates of their respective compositions. A double "V" 30° angle with a 1/8-in. land or root face and a root spacing of .045 in. describes the usual plate preparation for welding. For control purposes the welds are made inside a vacuum dry-box welding chamber, back-filled with an 80-20 argon, helium mixture. Later duplicate welds are made out in the open atmosphere using a trailing shield and backup inert gas coverage for protection from contamination. A constant potential dc power source automatically provides sufficient current to melt a 1/16-in.-diam electrode wire fed through a machine head at controlled rates of from 300 to 450 in./min, requiring 280 to 420 amps at 30 volts. By adjusting the carriage speed between 12 to 20 in./min the energy can be varied roughly between 25,000 and 45,000 j/in. of weld.

Preliminary results of DWT tests of welds in the three alloys show fracture toughness roughly equivalent to the base plate using single pass welds on both sides of the plate. Double pass welds seemingly have lower fracture toughness.

Charpy V specimens were prepared from all weld metal samples of these alloys and the data are shown in Fig. 31. Here again the notch fracture toughness of the weld metal is equivalent to the respective base plate. The tensile yield strengths of the two alloys tested (5Al-2.5Sn and 6Al-4V on 112 ksi and 126 ksi respectively) are also equivalent.

21

REFERENCES

1. Pellini, W.S., and Puzak, P.P., "Fracture
    Analysis Diagram Procedures for the Fracture-
    Safe Engineering Design of Steel Structures",
    NRL Report 5920, 15 March 1963; also, Welding
    Research Council Bulletin Series, WRC No. 88,
    May 1963

2. Pellini, W.S., and Puzak, P.P., "Factors that
    Determine the Applicability of High Strength
    Quenched and Tempered Steels to Submarine Hull
    Construction", NRL Report 5892, 5 December 1962.

3. Drennan, D.C., and Roach, D.B., "Properties of
    Maraging Steels", DMIC Memo 156, July 1962

4. Puzak, Lloyd, Lange, Goode, Huber, Dahlberg and
    Beachem, "Metallurgical Characteristics of High
    Strength Structural Materials (First Quarterly
    Report)", NRL Memo Report 1438, 30 June 1963

5. ASTM Materials and Research Standards, Vol. 1,
    No. 5, May 1961

TABLE I

CHEMICAL COMPOSITIONS OF SPECIALLY ROLLED AND HEAT TREATED HY-80 STEELS

Cross-Roll	Y.S.*	Composition - wt. %								
		C	Mn	Si	P	S	Ni	Cr	Mo
Straight	112	.1	.32	.33	.006	.012	3.20	1.66	.70
Straight	132	.20	.35	.32	.007	.010	3.20	1.69	.70
Straight	150	.18	.35	.33	.006	.010	3.16	1.62	.70
6.2 to 1	117	.18	.32	.35	.006	.010	3.12	1.62	.71
6.2 to 1	134	.19	.35	.31	.008	.011	3.16	1.64	.71
6.2 to 1	157	.19	.32	.33	.006	.013	3.28	1.69	.70
3.8 to 1	118	.21	.32	.34	.006	.014	3.28	1.67	.70
3.8 to 1	134	.19	.35	.31	.006	.011	3.20	1.65	.70
3.8 to 1	156	.21	.32	.33	.006	.011	3.20	1.65	.74

* The HY-80 composition steels were Q&T heat treated to develop minimum yield strength levels of 110, 130, and 150 ksi.

TABLE II

TEST DATA FOR SPECIALLY ROLLED AND HEAT TREATED HY-80 STEELS

Cross-roll	Direction of Test*	0.505" Dia. Tension Test Data				Charpy-V at 30°F (ft-lb)	Drop-weight Tear at 30°F (ft-lb)
		0.2% Y.S. (ksi)	T.S. (ksi)	El. in 2" (%)	R.A. (%)		
Straight	Weak	112.6	134.9	16.5	48.3	42	2000
	Strong	111.9	130.6	21.5	71.5	86	6250
3.8 to 1	Weak	120.0	138.2	17.0	51.4	40	2000
	Strong	117.9	137.3	21.5	65.4	75	4500
6.2 to 1	Weak	112.6	137.9	16.5	51.9	41	2250
	Strong	116.7	136.4	20.0	52.0	75	4750
Straight	Weak	131.8	151.6	14.5	45.8	30	1250
	Strong	132.0	151.2	19.0	66.8	82	5750
3.8 to 1	Weak	133.1	150.2	16.3	54.7	42	2250
	Strong	134.3	151.4	18.3	63.9	71	4000
6.2 to 1	Weak	134.0	152.1	14.5	46.0	30	1500
	Strong	134.0	152.2	18.5	64.5	76	3750
Straight	Weak	151.0	166.4	14.0	49.2	28	1250
	Strong	150.1	165.3	17.3	64.3	60	4750
3.8 to 1	Weak	155.9	172.8	13.3	43.7	24	1250
	Strong	155.6	172.8	15.8	53.3	45	2750
6.2 to 1	Weak	158.0	175.6	12.5	41.3	23	1000
	Strong	156.6	175.2	17.0	54.6	48	3250

NOTE: Test direction is defined in terms of fracture path in specimen: i.e.,
"Weak"=specimen fracture parallel to principal (or final) rolling direction;
"Strong"=specimen fracture transverse to principal (or final) rolling direction.

TABLE III

CHEMICAL COMPOSITIONS OF MARAGING STEELS

(All steels aged 3 hours at 900°F)

Melt practice and type	Heat Size (Ton)	Anneal 1 Hour (°F)	Composition (Wt. %)						
			Ni	Cr	Co	Mo	Ti	Al	C
CEVM-12Ni-3Cr-3Mo	1	1700	12.0	3.00	---	3.15	.19	.13	.023
Air--12Ni-3Cr-3Mo	1	1900	12.0	2.85	---	3.20	.12	.19	.015
CEVM-12Ni-3Cr-3Mo	1/2	1500	11.8	3.35	---	3.65	.12	.15	.021
Air--12Ni-3Cr-3Mo	1/2	1500	12.3	3.54	---	3.15	.13	.12	.023
CEVM-10Ni-5Cr-3Mo	1/2	1500	10.0	5.39	---	3.45	.12	.26	.015
CEVM-12Ni-5Cr-3Mo	1	1900	12.0	4.91	---	3.15	.18	.21	.015
CEVM-18Ni-8Co-2Mo	1/2	1500	18.0	--	8.4	2.15	.16	.06	.011
CEVM-18Ni-9Co-3Mo	1	1500	18.0	--	8.7	3.38	.18	.09	.015
Air--18Ni-9Co-3Mo	1	1500	18.2	--	8.7	3.25	.16	.10	.007
CEVM-18Ni-8Co-5Mo	1/2	1500	17.4	--	7.7	5.20	.32	.10	.025
CEVM-18Ni-9Co-5Mo	1	1500	18.0	--	9.1	5.05	.76	.16	.007
Air--18Ni-7-1/2Co-5Mo	10	1500	18.3	--	7.4	5.30	.24	--	--

TABLE IV

TEST DATA FOR ONE-INCH MARAGING STEELS
(Aged 3 hours at 900°F)

Melt practice and Type	Direction of test*	0.505" Dia. Tension Test Data				Charpy-V at 30°F (ft-lb)	Drop-weight tear at 30°F (ft-lb)
		0.2% Y.S. (ksi)	T.S. (ksi)	El. in 2" (%)	R.A. (%)		
CEVM-12Ni-3Cr-3Mo (1-ton heat)	Weak	146.3	154.3	15.5	61.7	64	3750
	Strong	148.1	158.2	16.0	64.1	104	4250
Air--12Ni-3Cr-3Mo (1-ton heat)	Weak	152.4	161.9	14.5	61.7	51	3250
	Strong	150.2	162.1	15.8	62.2	66	3500
CEVM-12Ni-3Cr-3Mo (1/2-ton heat)	Weak	139.7	141.5	18.3	67.2	99	5500
	Strong	146.3	148.5	16.8	66.3	108	6750
Air--12Ni-3Cr-3Mo (1/2-ton heat)	Weak	148.0	151.3	16.3	63.9	73	3750
	Strong	144.9	148.5	17.5	64.0	82	5500
CEVM-10Ni-5Cr-3Mo (1/2-ton heat)	Weak	154.4	156.2	18.0	67.3	104	5750
	Strong	157.2	160.7	15.3	63.7	102	7250
CEVM-12Ni-5Cr-3Mo (1-ton heat)	Weak	162.5	174.8	14.3	60.0	57	3750
	Strong	161.9	175.2	15.0	63.1	84	4750
CEVM-18Ni-8Co-2Mo (1/2-ton heat)	Weak	155.6	163.6	15.3	67.4	96	3750
	Strong	158.6	163.3	15.3	66.8	109	4750
CEVM-18Ni-9Co-3Mo (1-ton heat)	Weak	204.2	212.2	12.0	59.8	33	1250
	Strong	199.7	208.4	13.3	62.7	45	1750
Air--18Ni-9Co-3Mo (1-ton heat)	Weak	201.3	209.0	12.0	57.6	34	1000
	Strong	200.7	208.7	12.3	57.8	36	1250
CEVM-18Ni-8Co-5Mo (1/2-ton heat)	Weak	259.6	266.1	9.5	49.0	22	750
	Strong	248.5	254.9	10.0	49.0	22	750
CEVM-18Ni-9Co-5Mo (1-ton heat)	Weak	279.8	293.7	8.5	42.5	14	<500
	Strong	272.8	292.1	8.8	43.1	18	<500
Air--18Ni-7-1/2Co-5Mo (10-ton heat)	Weak	235.5	245.7	7.0	29.2	18	<500
	Strong	229.1	240.3	9.0	--	22	<500

*NOTE: Test direction is defined in terms of fracture path in specimen: i.e.,
"Weak"=specimen fracture parallel to principal (or final) rolling direction;
"Strong"=specimen fracture transverse to principal (or final) rolling direction.

TABLE V

LOW-CYCLE FATIGUE TEST DATA
FOR HY-80 STEEL, Ti-6Al-4V TITANIUM, AND 2024 ALUMINUM

Material	Initial Cycles	Final Cycles	Cycle Interval	Strain Range (μ in. /in.)	Average Crack Length (in.)	Crack Growth Rate (μ in. /cycle)	$CR/(CL)^{\frac{2}{3}}$
HY-80	1550	3100	1550	6730	0.170	57	186
(E84-1)	3100	4400	1300	4800	0.237	35	92
5% Crack	4400	5500	1100	6700	0.308	88	193
HY-80	1550	3100	1550	6730	0.294	65	147
(E84-1)	3100	4400	1300	4800	0.371	39	75.5
10% Crack	4400	5500	1100	6700	0.456	108	182
HY-80	0	1600	1600	6730	0.289	58	133
(E84-11)	1600	2300	700	4830	0.358	31	62
10% Crack	2300	4500	2200	6730	0.470	111	185
	4500	6100	1600	7820	0.806	260	299
	6100	6600	500	6730	1.170	220	198
2024-2	0	2000	2000	7100	0.298	31	68
Aluminum	2000	4100	2100	5260	0.322	7	16
10% Crack	4100	5000	900	8370	0.431	205	360
	5000	6650	1650	7100	0.536	52	79
	6650	6850	200	9850	0.675	822	1070
Ti-6Al-4V	2500	3100	600	9800	0.324	64	134
Titanium	3100	4500	1400	7600	0.352	16	33
(T5-2)	3800	4700	900	7600	0.358	29	59
10% Crack	4700	4900	200	11,800	0.390	224	420
	5750	7000	1250	5600	0.433	13	23
	10,850	12,000	1150	7000	0.455	23	38.5
	12,000	12,200	200	12,700	0.502	323	523
	12,000	13,000	1000	12,700	0.664	407	534
	13,800	14,000	200	14,000	1.032	965	950

TABLE VI
TENSILE PROPERTIES OF MATERIALS IN
LOW-CYCLE FATIGUE STUDY

Material	Alloy	UTS (ksi)	YS 0.2% (ksi)	Elong. (%)	Modulus of Elasticity	Total Strain at 0.2% YS (in./in.)
Steel	HY-80	105	88	23.5	30×10^6	0.485
Titanium	Ti-6Al-4V	131	126	12.5	18×10^6	0.90
Aluminum	2024	68	47	19	11×10^6	0.61

TABLE VII
CRACK GROWTH RATES FROM LOW-CYCLE FATIGUE
OF HY-80 STEEL, Ti-6Al-4V, AND 2024 ALUMINUM

Alloy	Strain Range Exponent M	Crack Growth Rate for 1-in. Long Crack μ in./cycle	
		± 40 ksi Stress	$E_p = 0.01\%$
HY-80	2.5	15	170
Ti-6Al-4V	5	45	1250
2024 Aluminum	7	140	960

TABLE VIII
TENSILE PROPERTIES OF SOME TITANIUM ALLOY PLATES
AT ROOM TEMPERATURE

Plate No.	Nominal Composition	Plate Condition	YS (ksi)	UTS (ksi)	RA (%)	Elong (%)
T- 7	Ti-5Al-2.5Sn	As Rolled	125.5	130.5	13	15
T- 8	Ti-6Al-4V	As Rolled	123	136.5(L) 139 (T)	15	20
T- 9	Ti-13V-11Cr-3Al	As Rolled	125 (L) 128.5(T)	135.5(L) 135.5(T)	6	9
T-19	Ti-8Al-1Mo-1V	As Rolled	123.4	132	25.5	14
		H.T.(vac) 1825°F/1hr	107.9	125.7	35.6	15.9
		H.T. 1825°F/2hr/ AC	112	126.7	29.6	15
T-20	Ti-6Al-4Sn-1V	As Rolled	130	133	33	10
		H.T.(vac) 1800°F/1hr	108.5	113.5	48.6	17.7
		H.T. 1800°F/2hr/ AC	110.4	114	45.1	18.4
T-21	Ti-6Al-6V-2.5Sn	As Rolled	150	152	42	10
		H.T.(vac) 1660°F/1hr	139	147.7	51.1	13.9
		H.T.(vac) 1660°F/2hr/ AC	137.4	146.9	41.3	13.7
T-22	Ti-6Al-2Mo	As Rolled	125	128	42	9
		H.T.(vac) 1800°F/1hr	115.6	123.7	48.8	14.3
		H.T. 1800°F/2hr/ AC	116.9	122.5	41.7	14.3
T-26	Ti-7Al-2Cb-1Ta	As Cast Plate	93.2	96.5	32.2	9.3
T-33*	Ti-7Al-2Cb-1Ta	Hot Rolled & Annealed	106.6(L) 111.7(T)	126.0(L) 130.5(T)	29.3(L) 28.1(T)	15 (L) 14 (T)

* Tensile Data for Plate T-33 is Producers' Data

29

TABLE IX

DROP-WEIGHT TEAR TEST ENERGY ABSORPTION VALUES OF SOME TITANIUM ALLOYS

Plate No.	Nominal Composition	Plate Condition	Energy Absorption (ft-lbs)		Remarks
			RW	WR	
T- 7	Ti-5Al-2.5Sn	As Rolled H.T. 1900°F/1hr/AC	<2000 <1000		
T- 8	Ti-6Al-4V	As Rolled H.T. 1900°F/1hr/AC	<1500 <1000		
T- 9	Ti-13V-11Cr-3Al	As Rolled	<1000		
T-19	Ti-8Al-1Mo-1V	As Rolled H.T. 1825°F/2hr/AC	1225	1225 2500	

T-20	Ti-6Al-4Sn-1V	As Rolled
		H.T.
		  1800°F/1hr/AC
		H.T.
		  1800°F/2hr/AC
			2250	<1500
				2750
				
				<2500
					Suspect-
					evaluation
					continuing

T-21	Ti-6Al-6V-2.5Sn	As Rolled H.T. 1660°F/2hr/AC	950	950 1750	

T-22	Ti-6Al-2Mo	As Rolled
		H.T.
		  1800°F/1hr/AC
		H.T.
		  1800°F/2hr/AC
			1750	2000
				2750
				
				3125	

T-26	Ti-7Al-2Cb-1Ta	As Cast Plate As Rolled		 ~3250	~3750 ft-lbs
T-33	Ti-7Al-2Cb-1Ta	As Received (Processing Un- known except Hot-Rolled, Annealed & Pickled)	2750		Under bead crack- Suspect

TABLE X

SOME MECHANICAL PROPERTIES OF PLATES T-17 AND T-23

Plate No.	Nominal Composition	Condition Tested	YS (ksi)	DWTT (ft-lbs)	C_v(32°F) (ft - lbs)
T-17	Unalloyed Ti (High Interstitial)	As Rolled	83	660	15
T-23	Ti-8Al-2Cb-1Ta	1965°F/1hr /AC	112.5	<2000	32
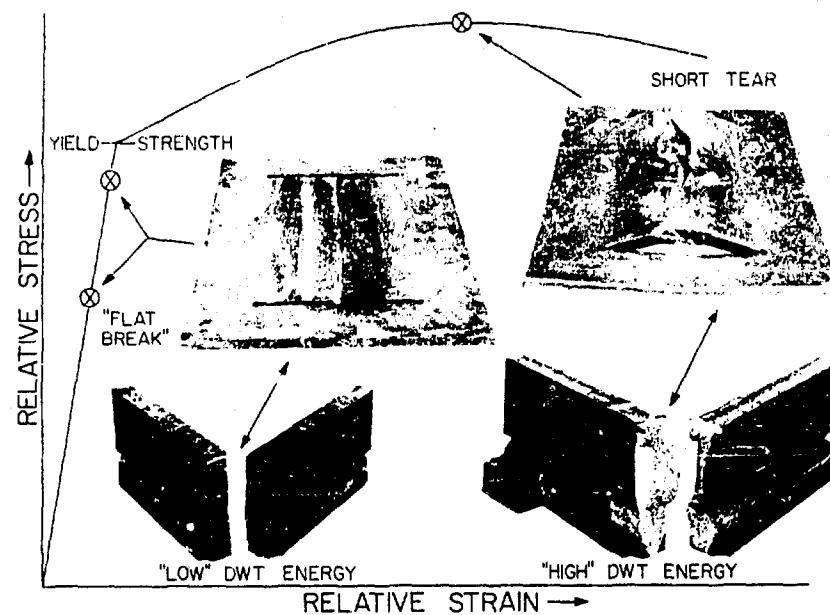
Fig. 1 - Features of explosion tear and drop-weight
tear specimens and procedures employed for frac-
ture toughness evaluations of heavy section, high
strength materials. The specimens illustrate the
extremes in performance obtained for steels tested
in the presence of a 2-in. crack.
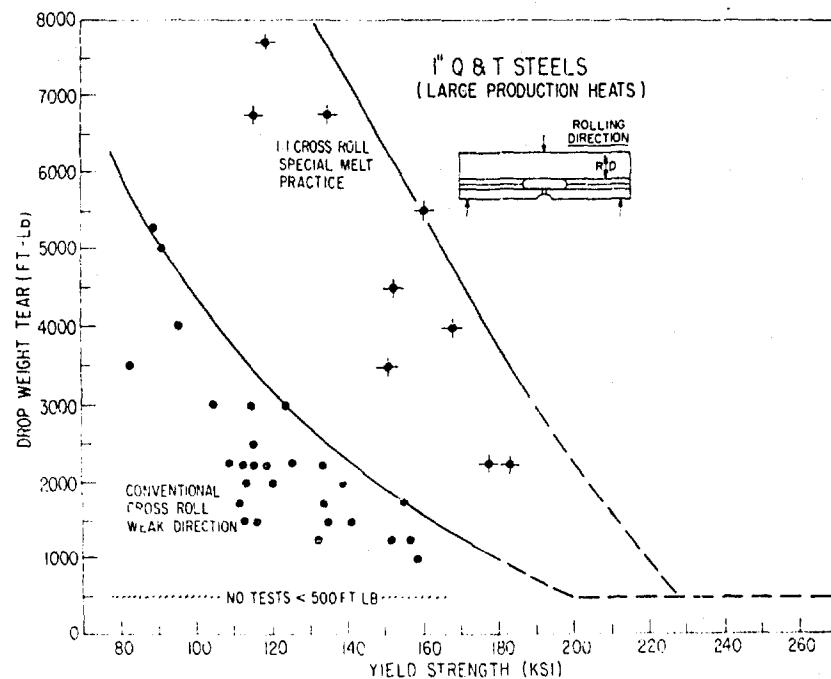
Fig. 2 - Illustrating drop-weight tear and yield
strength relationships for quenched and tempered
steels.
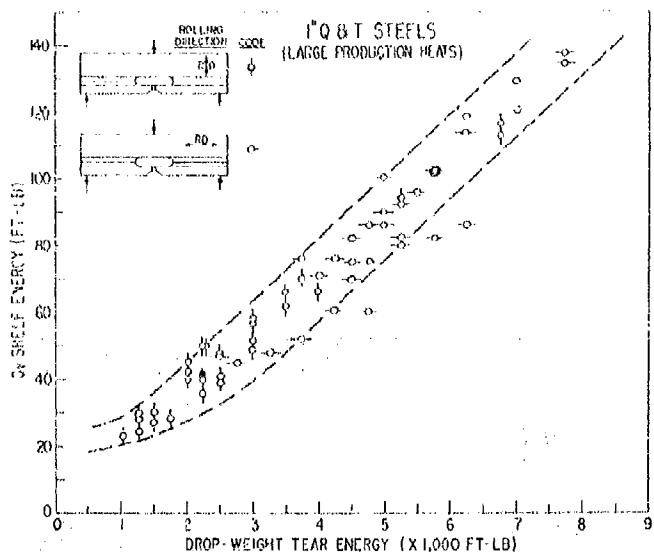
Fig. 3 - Correlation of drop-weight tear test
energy absorption values with Charpy V test
shelf energy values for quenched and
tempered steels.
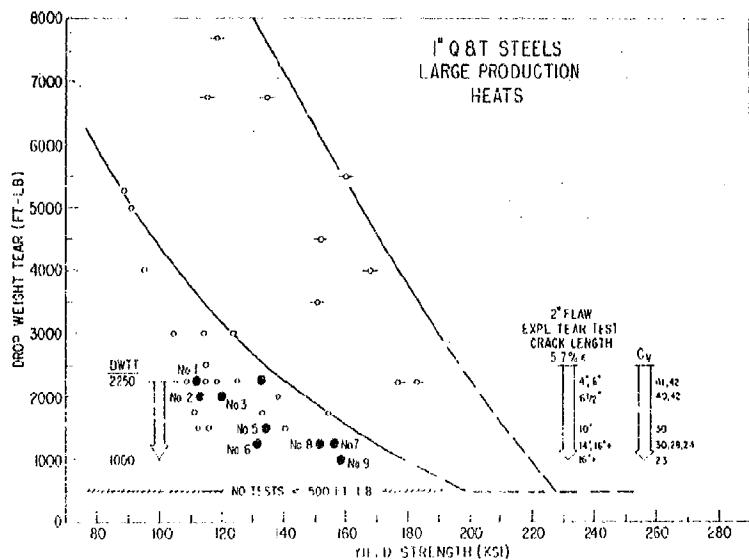
Fig. 4 - Drop-weight tear and yield strength re-
lationships for quenched and tempered steels.
The values obtained for steel Nos. 1 to 9 are
highlighted to indicate significance of drop-weight
tear test energy values to explosion tear test
performance in the presence of a 2-in. crack as
shown in Fig. 5.

NO.1 DWTT 2250 FT.LB.	NO.4 DWTT 2250 FT.LB.	NO.7 DWTT 1250 FT.LB.
NO.2 DWTT 2000 FT.LB.	NO.5 DWTT 1500 FT.LB.	NO.8 DWTT 1250 FT.LB.
NO.3 DWTT 2000 FT.LB.	NO.6 DWTT 1250 FT.LB.	NO.9 DWTT 1000 FT.LB.
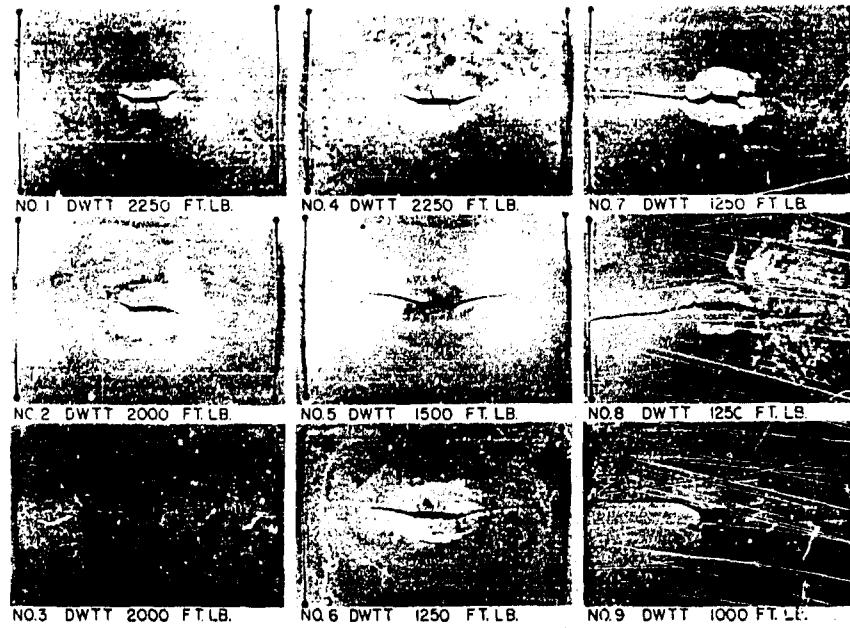
Fig. 5 - Explosion tear test specimens of specially processed HY-80 steel composition, heat-treated to HY-110 to HY-155 strength levels, illustrating the change in fracture toughness of steels with increasing drop-weight tear energies from 1000 to 2250 ft-lbs.
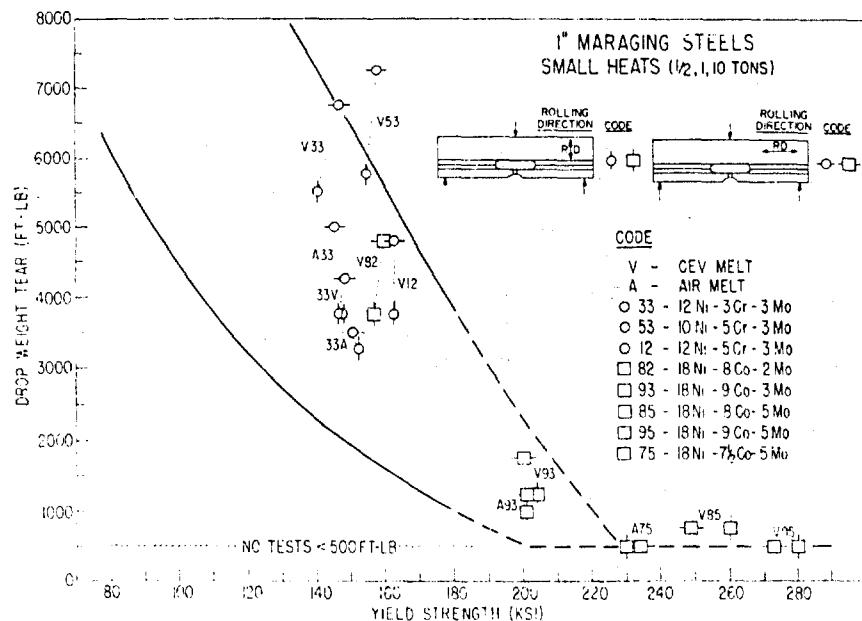
Fig. 6 - Illustrating drop-weight tear and yield strength relationships for maraging steels as compared to the practicable upper limit curves for toughness established with quenched and tempered steels.
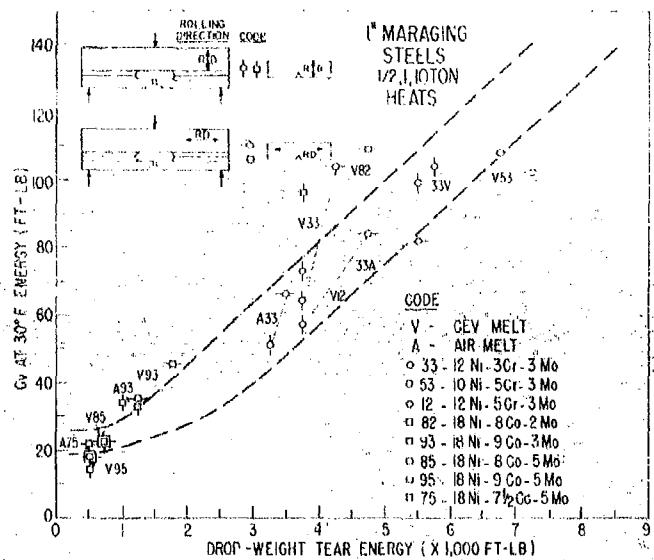
Fig. 7 - Correlation of drop-weight tear test energy absorption values with Charpy V tests at 30°F for maraging steels as compared to data band curves established for quenched and tempered steels.
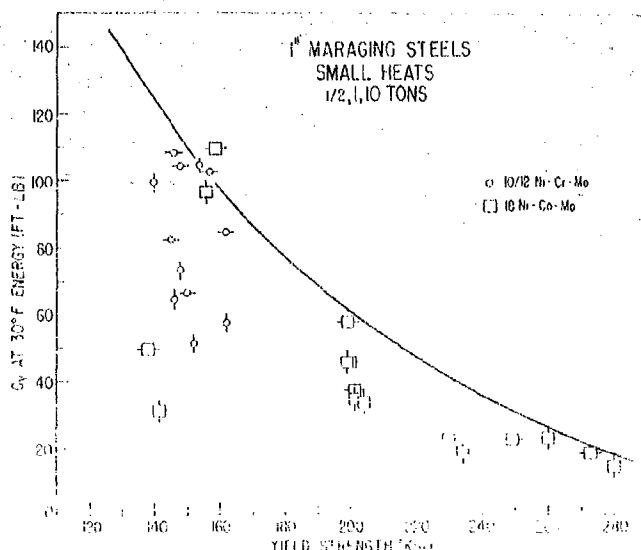
Fig. 8 - Charpy V and yield strength relationships for maraging steels.

NO.11 DWTT 3250 FT. LB.

NO.10 DWTT 5500 FT. LB.

NO.13 DWTT 1000 FT. LB.

NO.12 DWTT 1250 FT. LB.
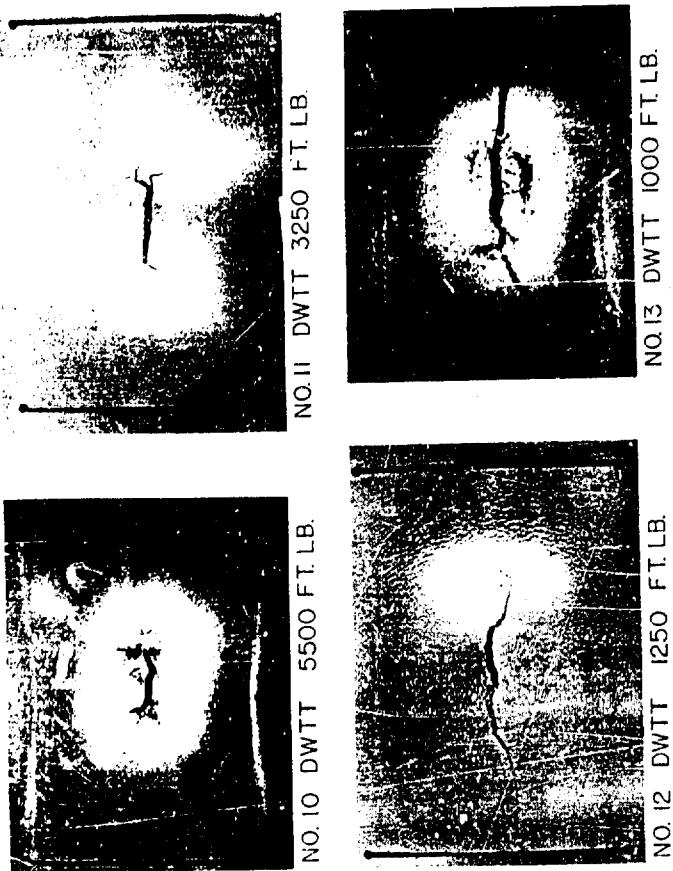
Fig. 10 - Explosion tear test specimens of maraging steel Nos. 10 to 13 (see Fig. 9), illustrating high fracture toughness of steels with more than 3000 ft-lb drop-weight tear energies (top) and complete fractures for steels of 1000 and 1250 ft-lb drop-weight tear energies (bottom). The presence of large lamination in steel No. 12 precluded the development of a complete rupture in this specimen.
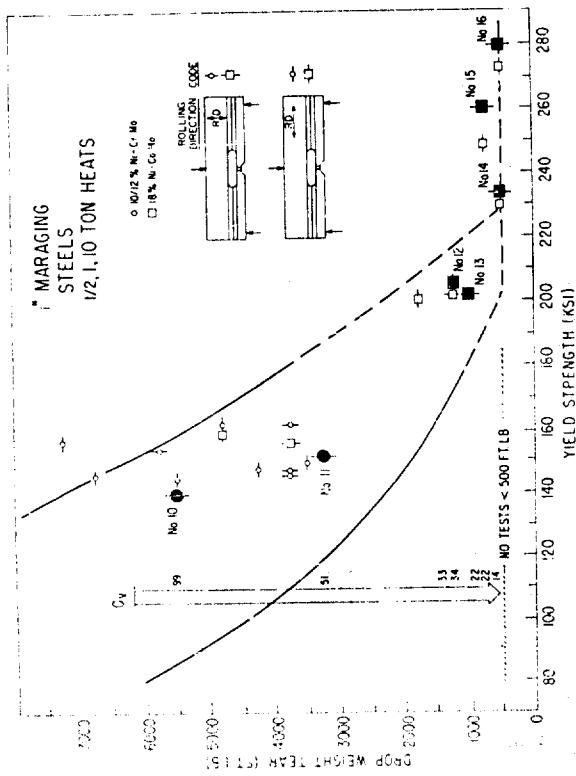
Fig. 9 - Drop-weight tear and yield strength relationships for maraging steels. The values obtained for steel Nos. 10 to 16 are highlighted to indicate significance of drop-weight tear test energy values to explosion tear test performance in the presence of a 2-in. crack as shown in Figs. 10 and 11.

NO. 15 DWTT 750 FT. LB.   NO. 16 DWTT   500 FT. LB.

Fig. 11 - Explosion tear specimens of maraging steel
Nos. 15 and 16 (see Fig. 9), illustrating "flat" break
performance with elastic levels of loading for steels
of 500 and 750 ft-lb drop-weight tear energies.
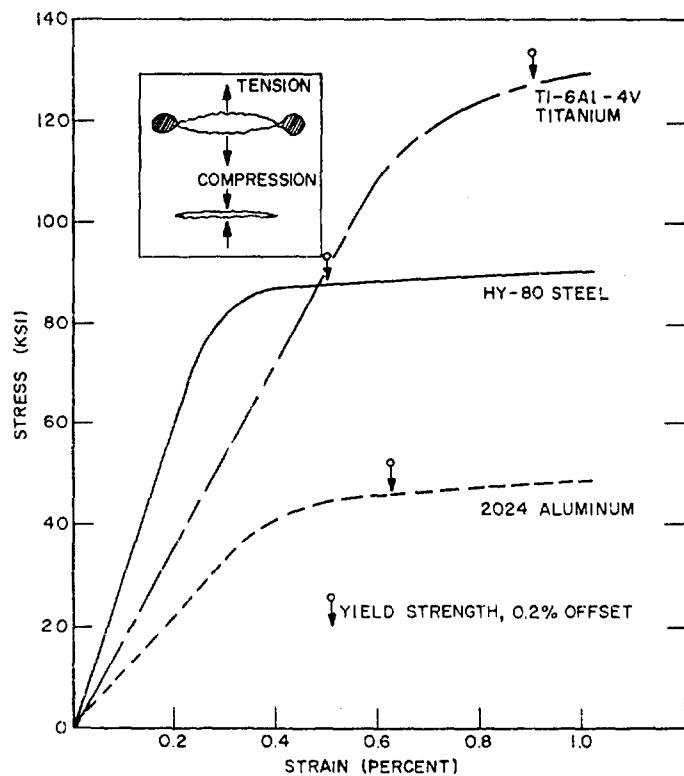
Fig. 12 - Stress-strain relationship in
tensile test for HY-80 steel, Ti-6Al-4V
titanium, and 2024 aluminum. Plastic
strain zones at tips of fatigue cracks
are illustrated.
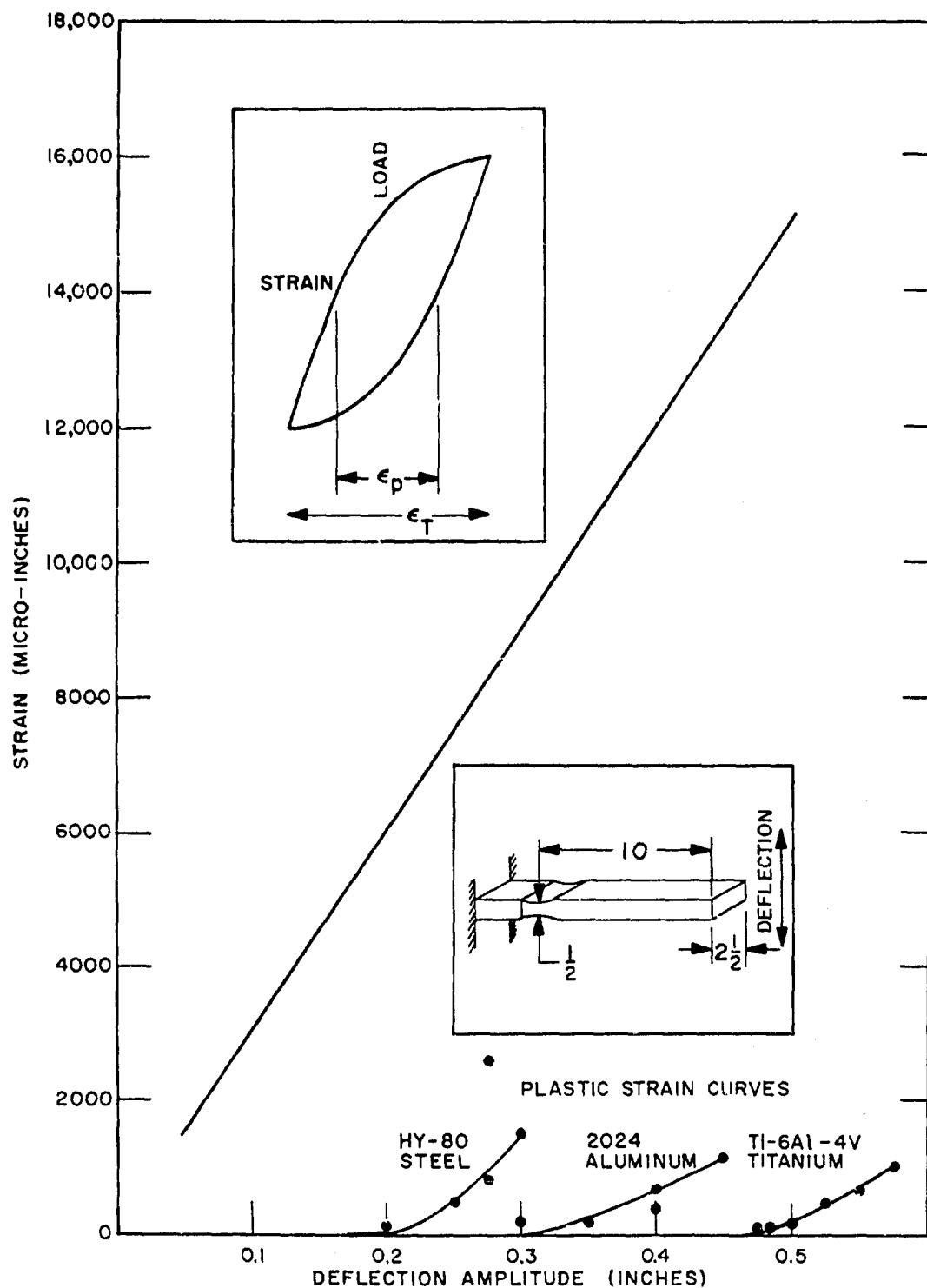
Fig. 13 - Relationship between strain range, plastic strain and
deflection in low-cycle fatigue specimen. The specimen and a
typical load-strain hysteresis loop are illustrated.
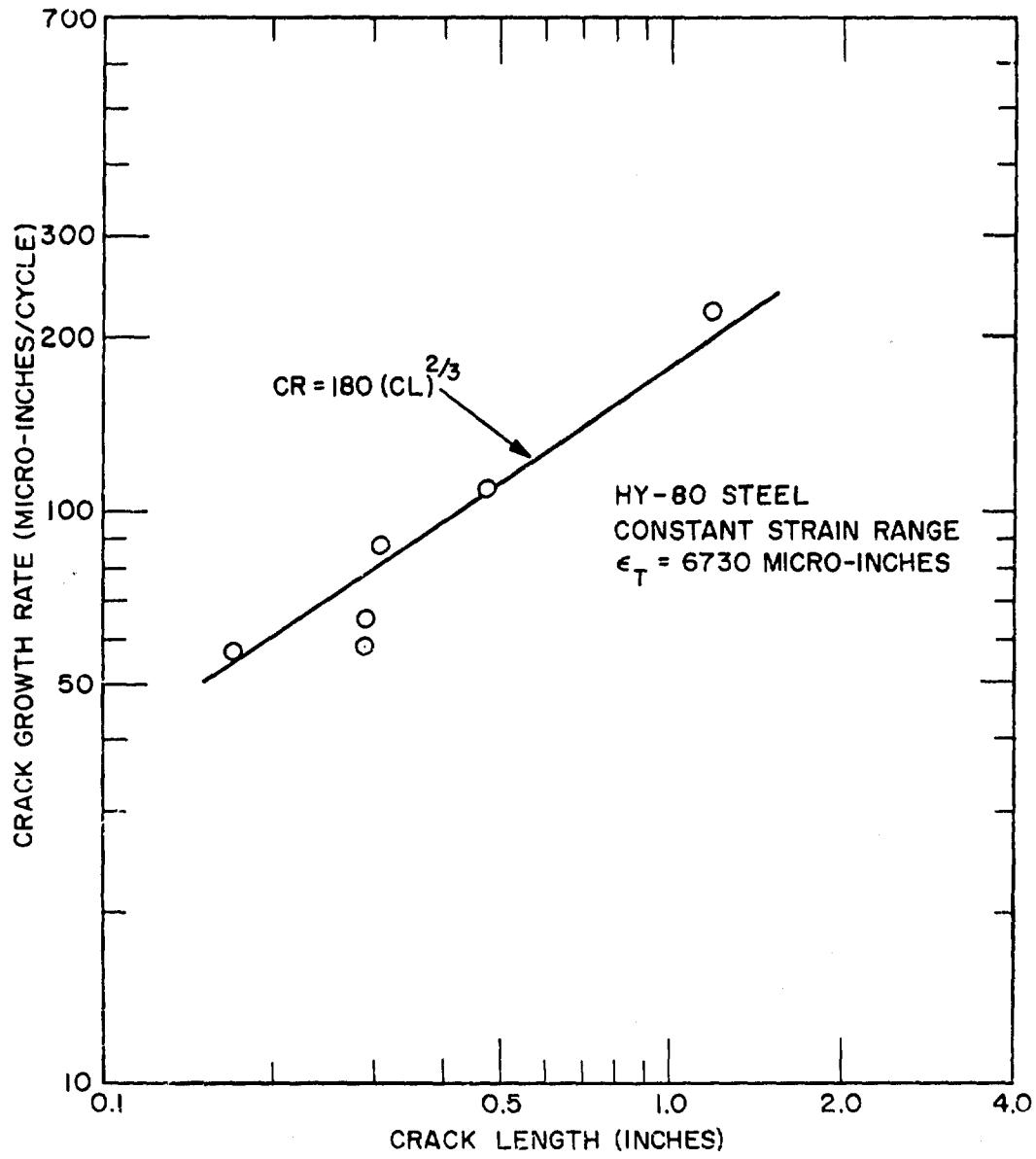
Fig. 14 - Effect of total crack length on crack growth
rate for HY-80 steel.

$$CR/_{(CL)^{2/3}} = K\epsilon_T^m$$

FOR STEEL, m = 2.5
FOR TITANIUM, m = 5
FOR ALUMINUM, m = 7

STEEL
TITANIUM
ALUMINUM

○ HY-80 STEEL
△ TI-6Al-4V TITANIUM
□ 2024 ALUMINUM
● → STRAIN RANGE EQUIVALENT TO ± 40 KSI
○ → ϵ = 0.01%

CR/$_{(CL)^{2/3}}$

STRAIN RANGE (MICRO-INCHES/INCH)

2000
1000
500
200
100
50
20

2000
5000
10,000
30,000
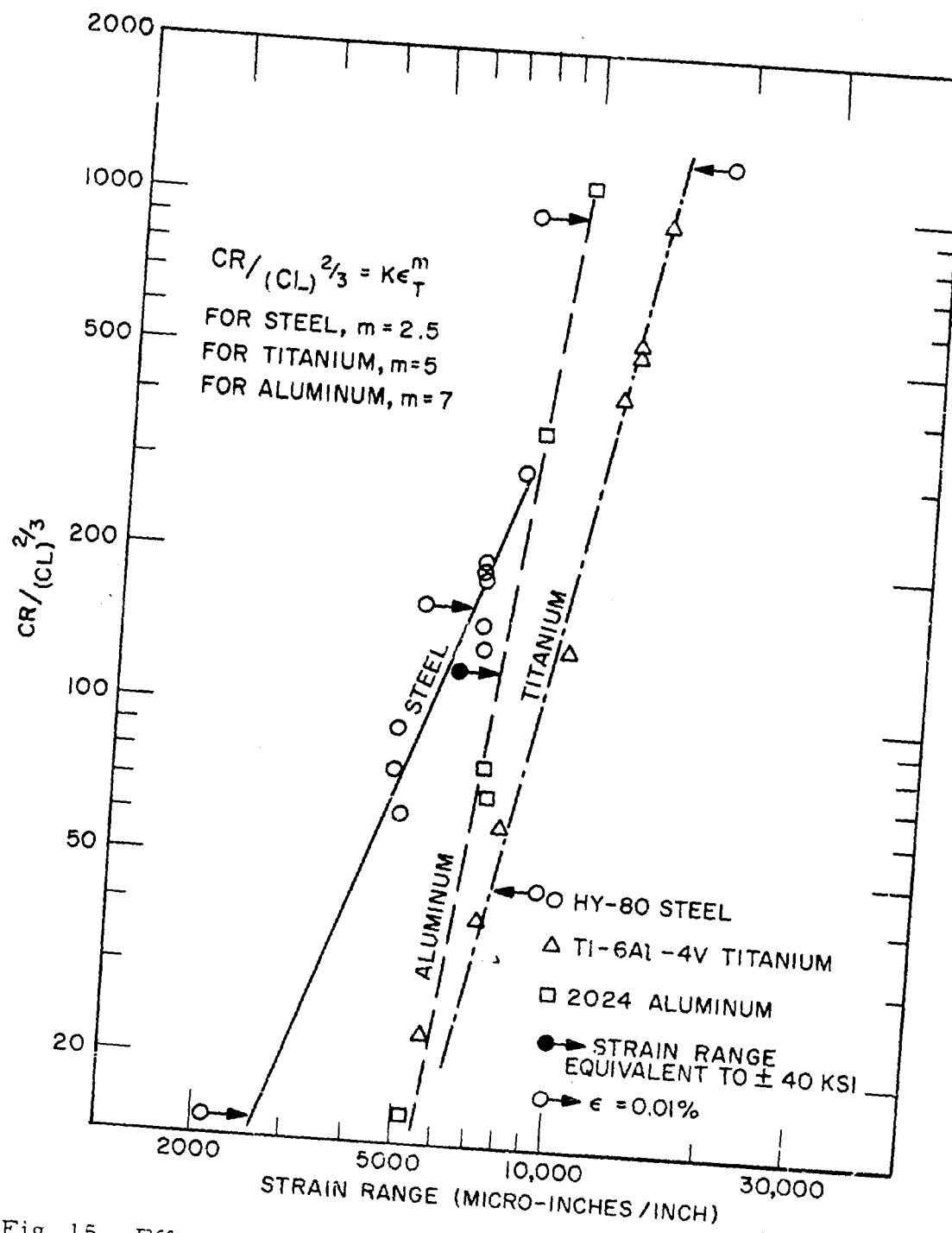
Fig. 15 - Effect of strain range on crack growth rate in HY-80 steel, Ti-6Al-4V titanium, and 2024 aluminum.
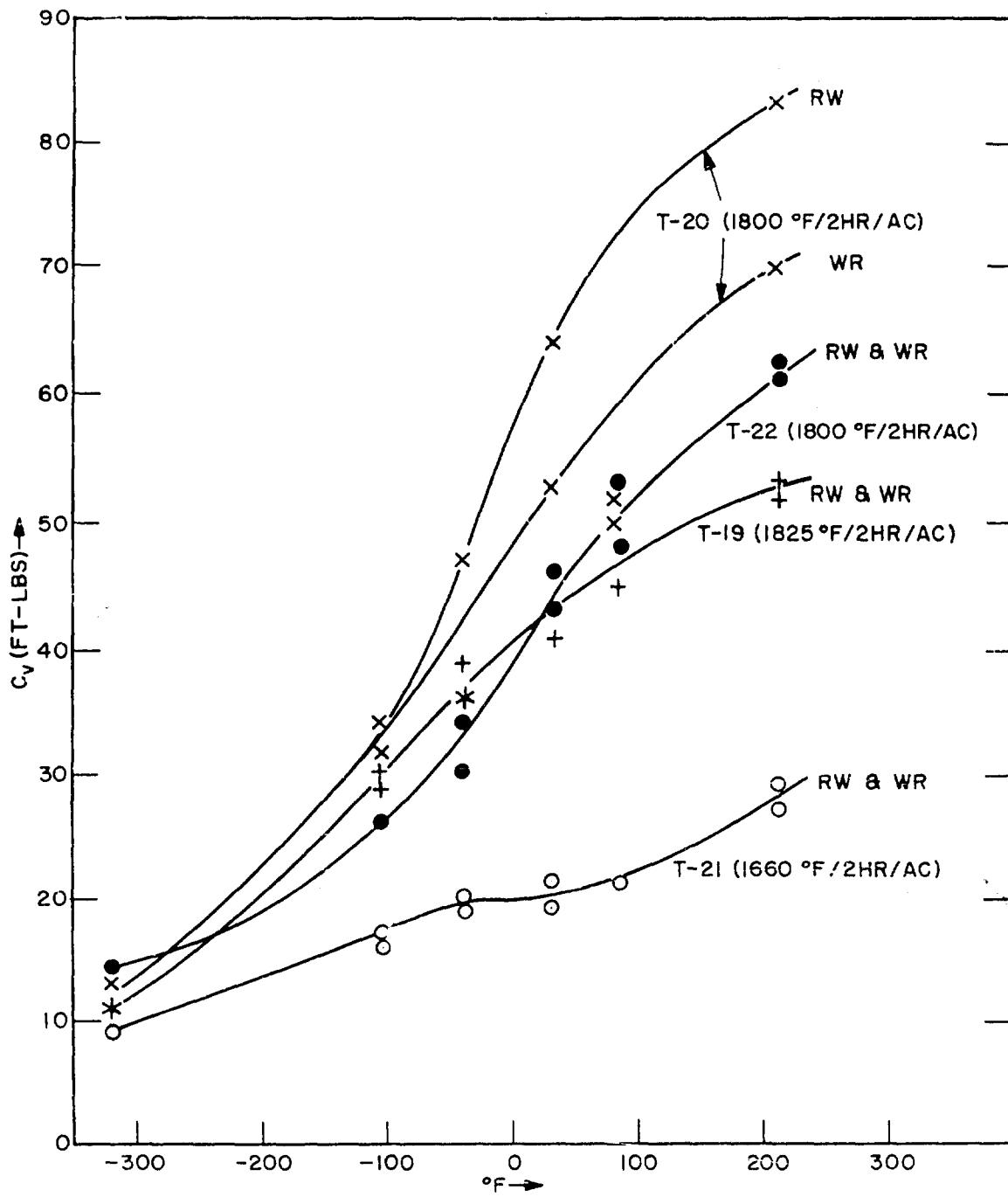
Fig. 16 - Charpy V-notch properties of heat-treated drop-weight tear
test specimens of plates T-19, T-20, T-21, and T-22.
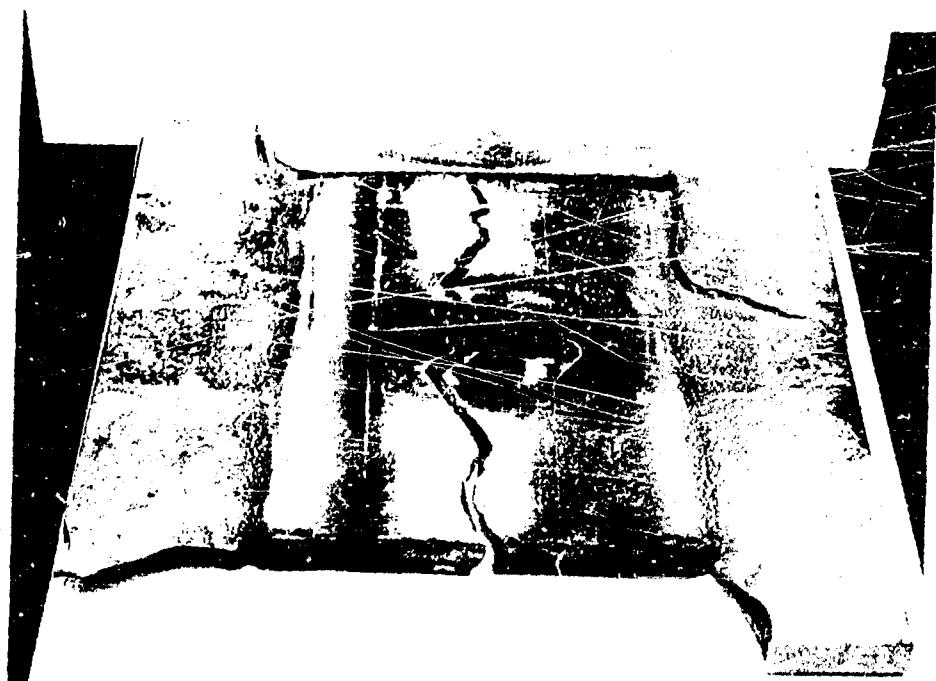
Fig. 17 - Explosion tear test fracture in 1-in. thick unalloyed titanium plate T-17 at 0% strain deformation with a 2-in. flaw.

Fig. 18 - Explosion tear test fracture in 1-in. thick Ti-8Al-2Cb-1Ta plate T-23 at 5-7% strain deformation with a 2-in. flaw.
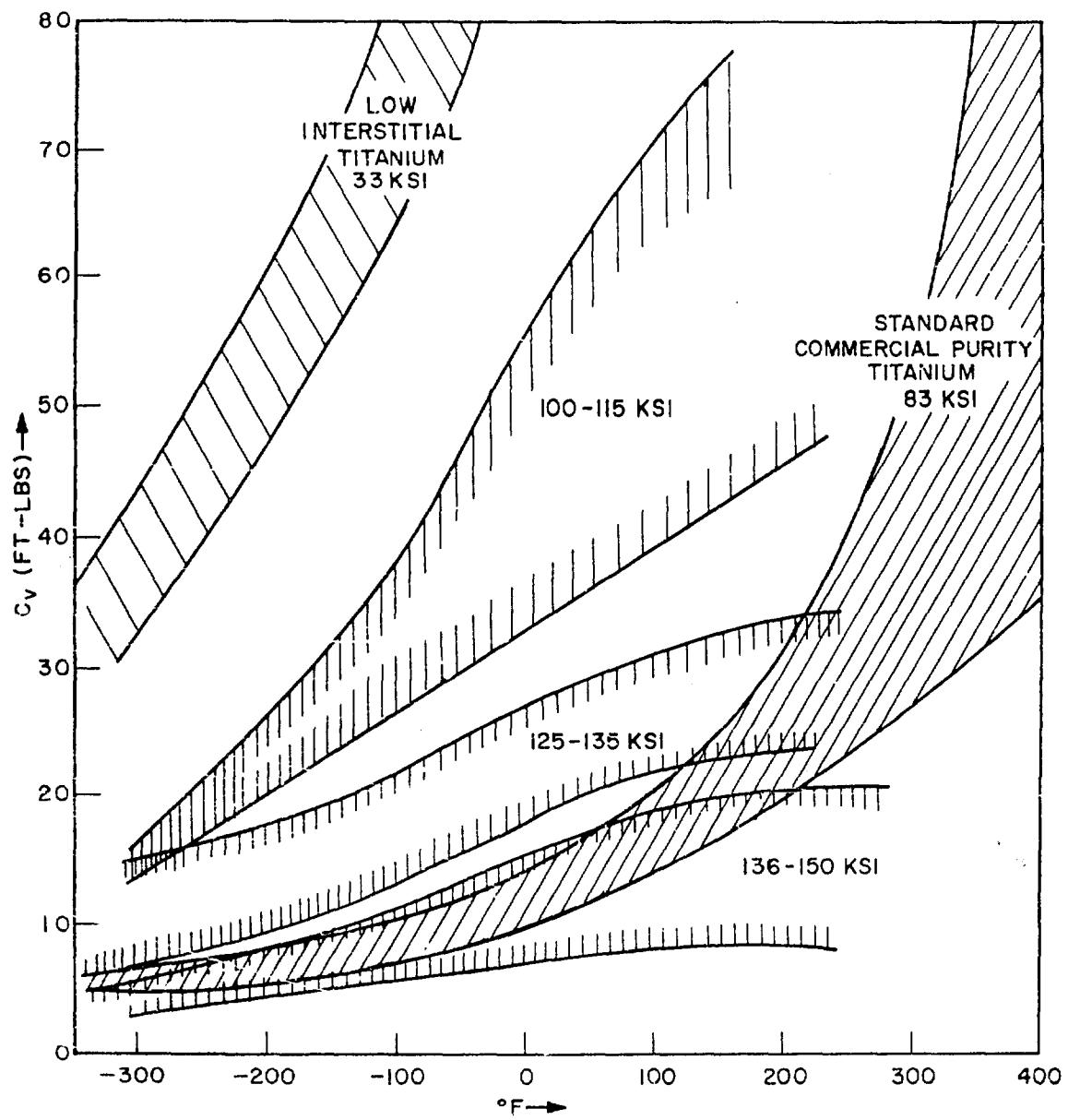
Fig. 19 - Fracture toughness of titanium alloys at various yield
strength levels as measured by the Charpy V-notched test.
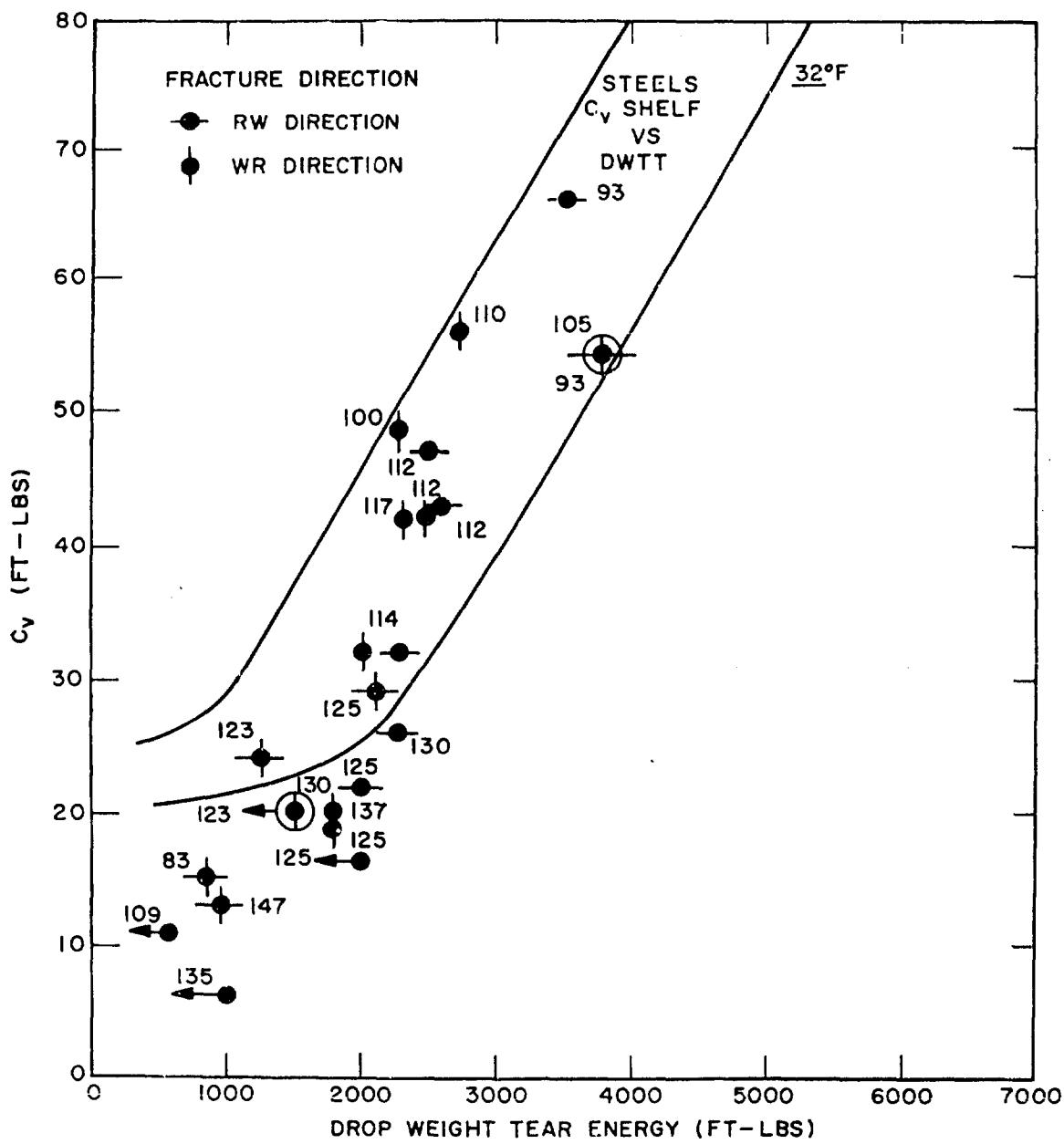
Fig. 20 - Correlation of drop-weight tear energy absorption values with Charpy V energy values of 1-in. thick titanium and titanium alloy plate.
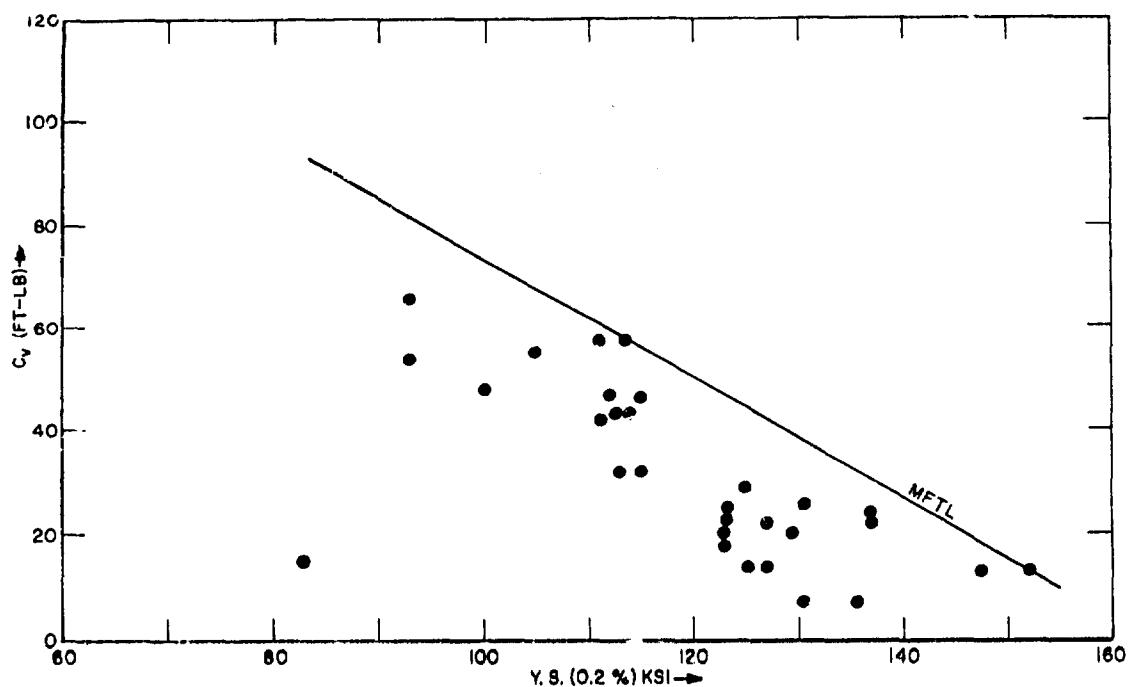
Fig. 21 - Correlation of Charpy V-notch energy with yield strength
for titanium and titanium alloy plate.
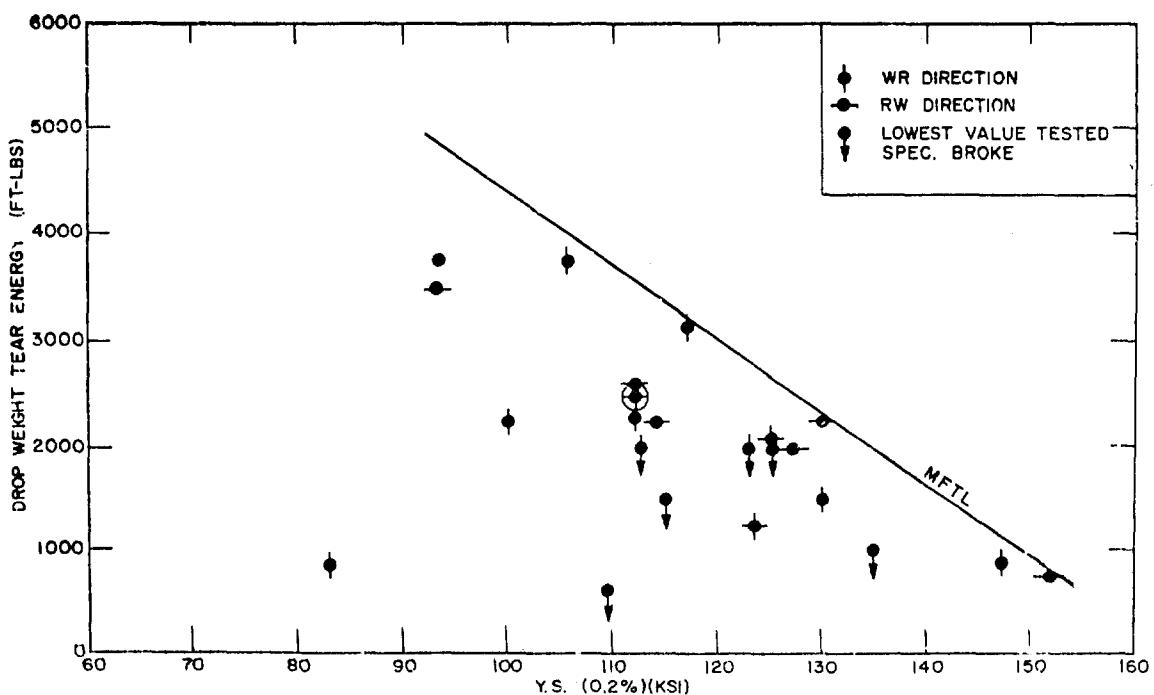
Fig. 22 - Correlation of drop-weight tear energy with yield strength
for titanium and titanium alloy plate.
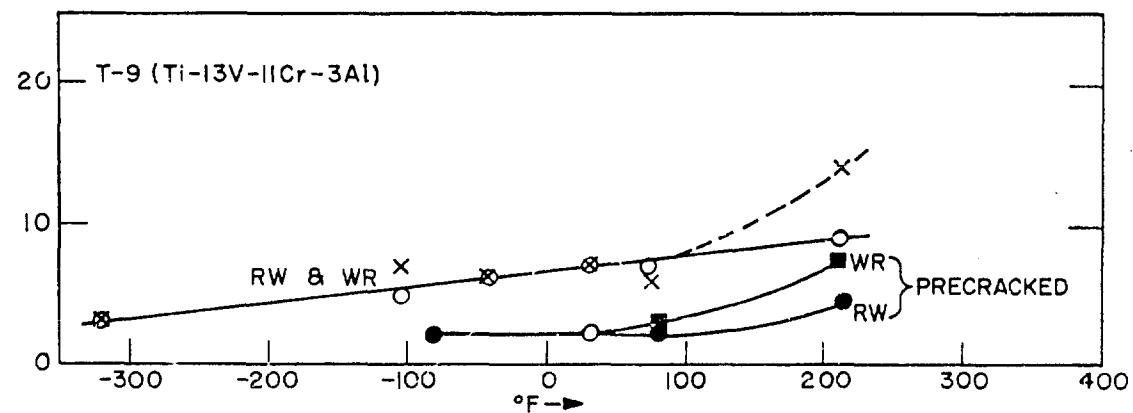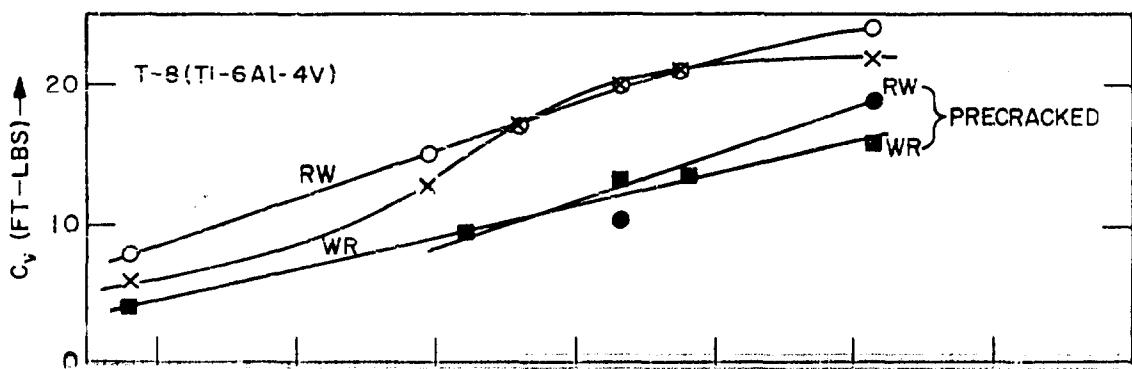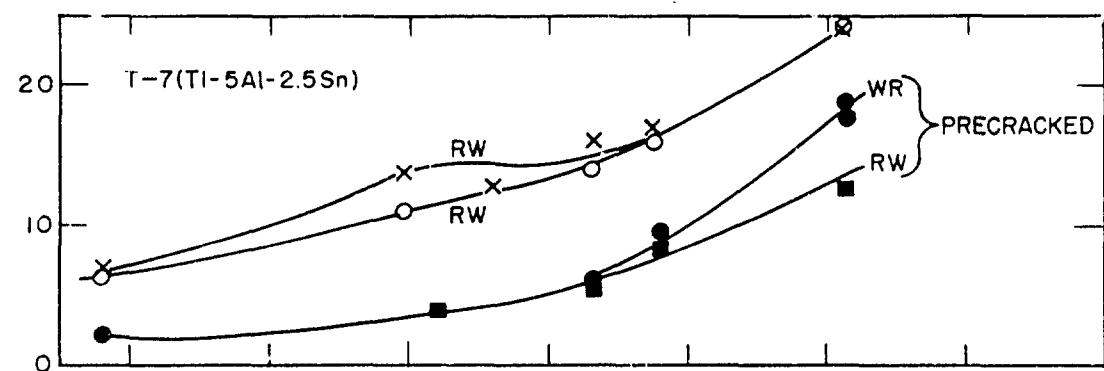
Fig. 23 - Standard and pre-crack Charpy V-notch properties of plates
T-7, T-8, and T-9 in the as-rolled condition.
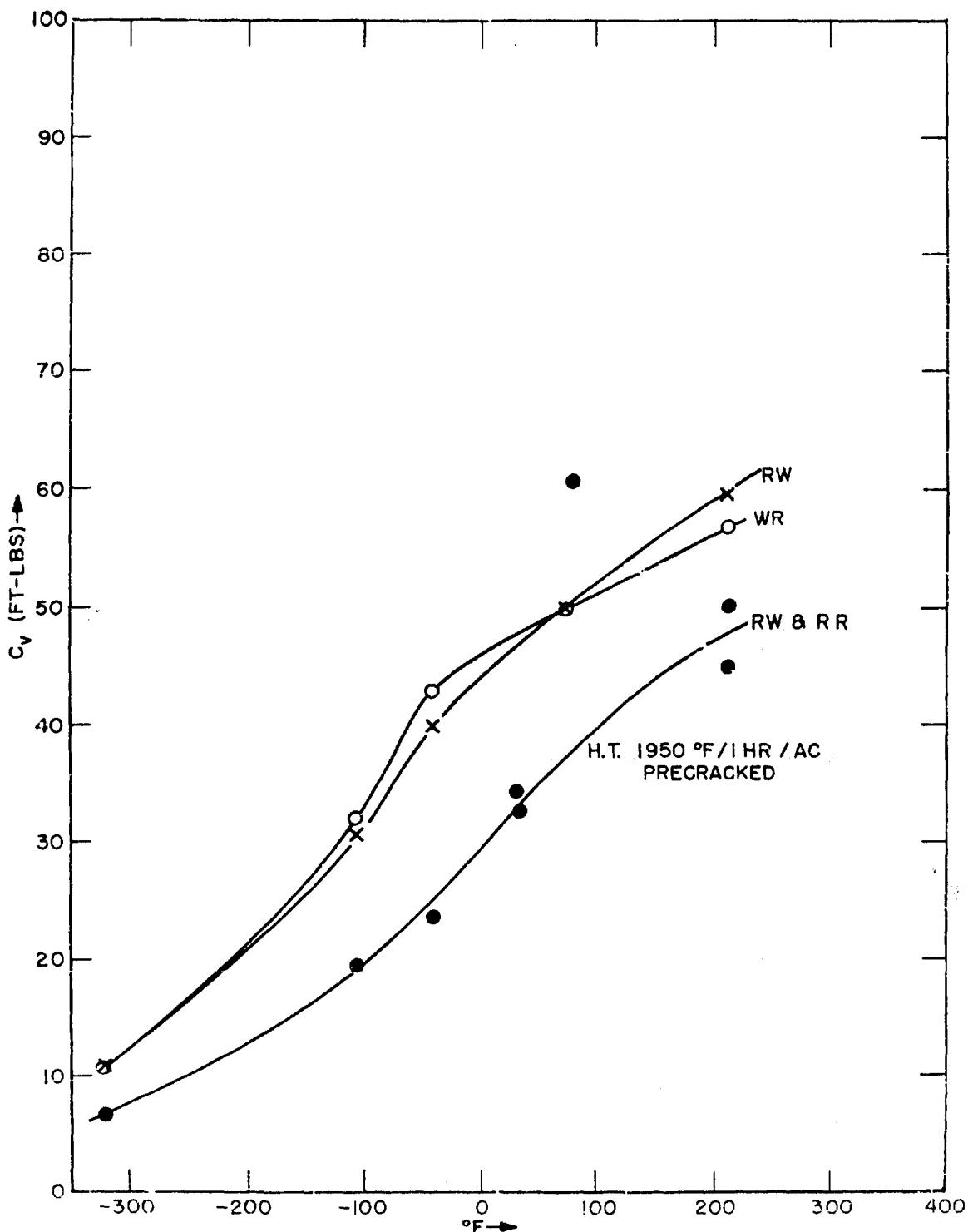
Fig. 24 - Standard and pre-crack Charpy V-notch properties of plate
T-11 (Ti-8Al-2Cb-1Ta) heat-treated at 1825°F and 1 hour in argon
and air-cooled.
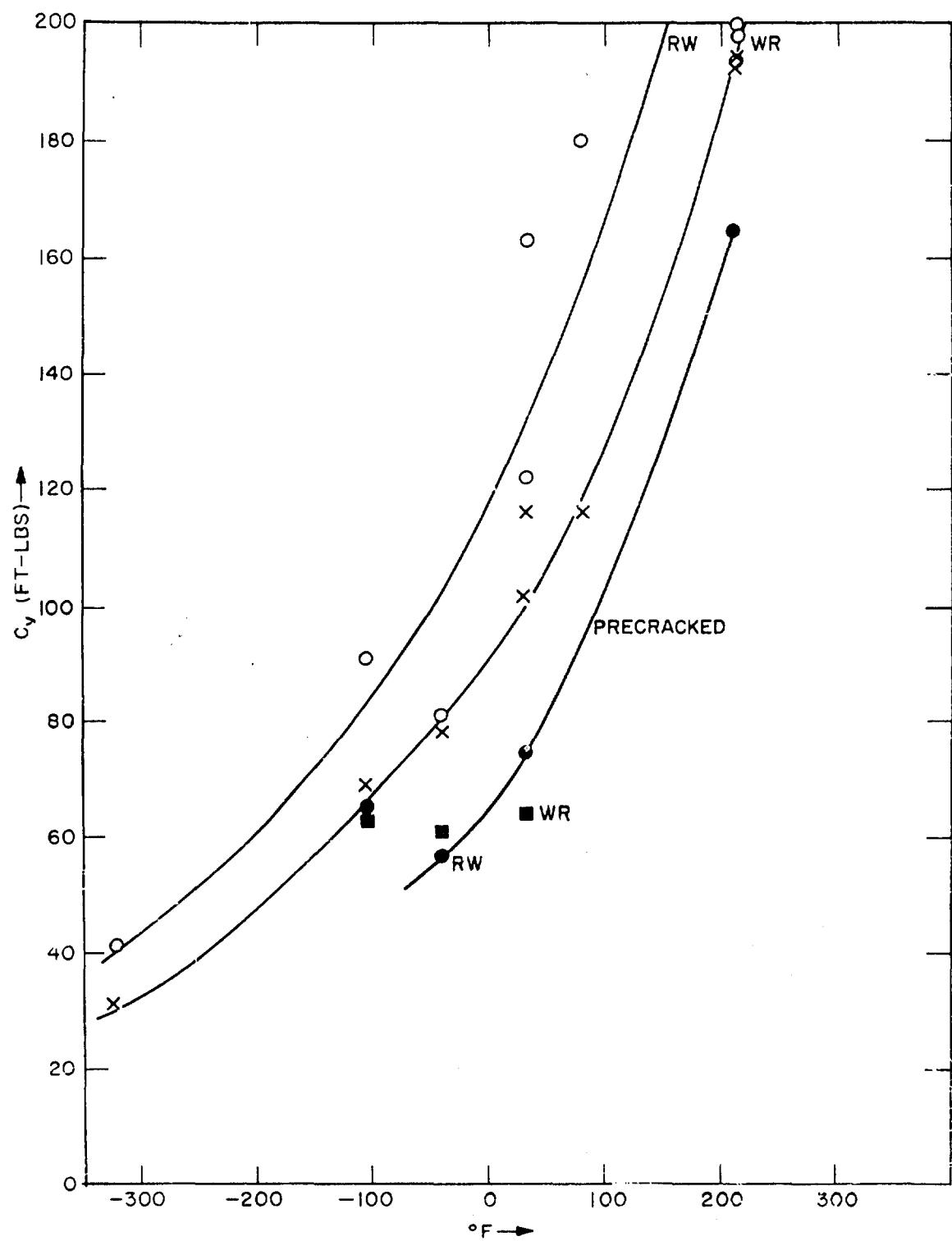
Fig. 25 - Standard and pre-crack Charpy V-notch properties of plate
T-16 (unalloyed Ti) in the as-rolled condition.
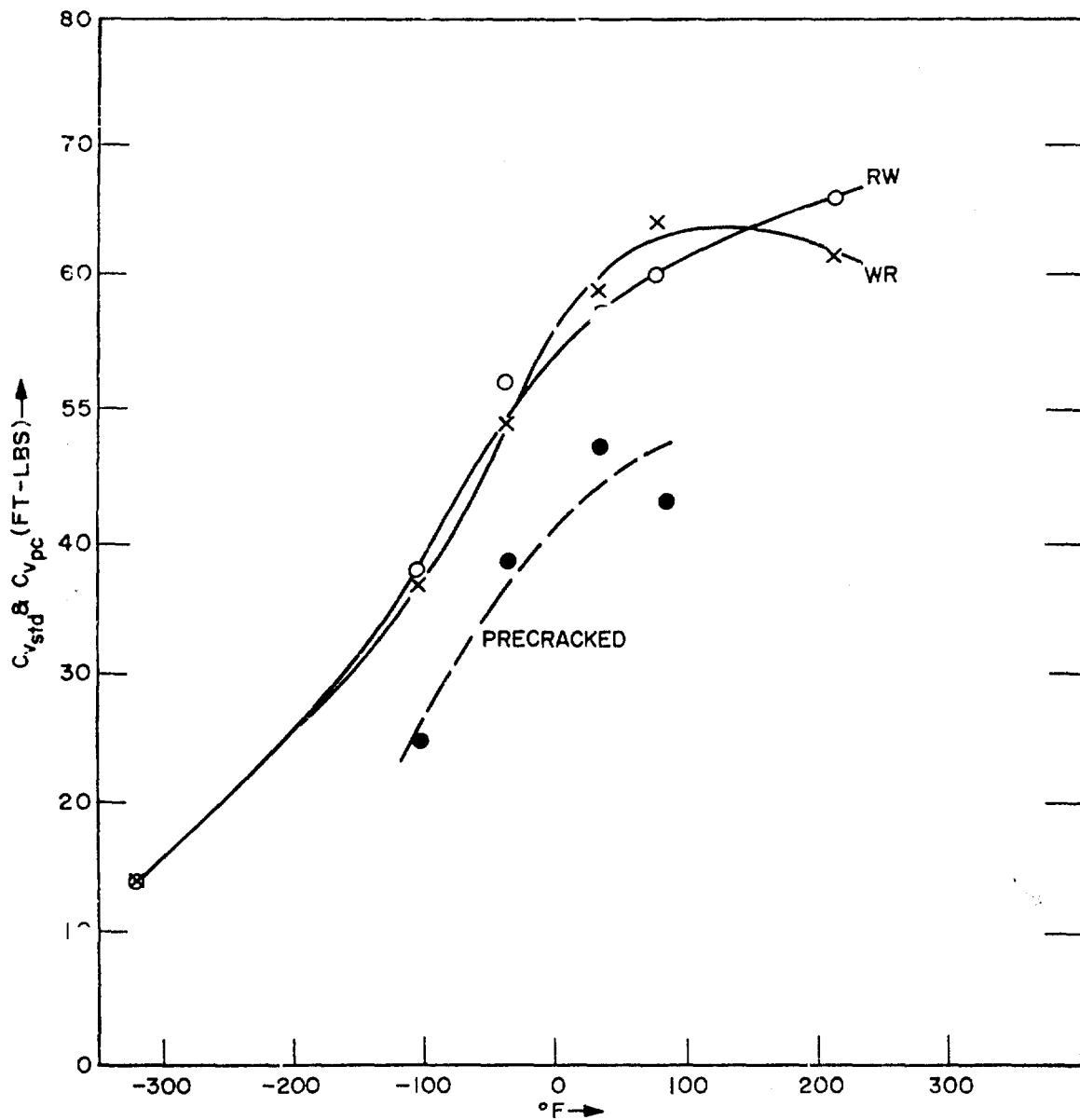
Fig. 26 - Standard and pre-crack Charpy V-notch properties of plate
T-19 (Ti-8Al-1Mo-1V) heat-treated at 1825°F for 1 hour in vacuum.
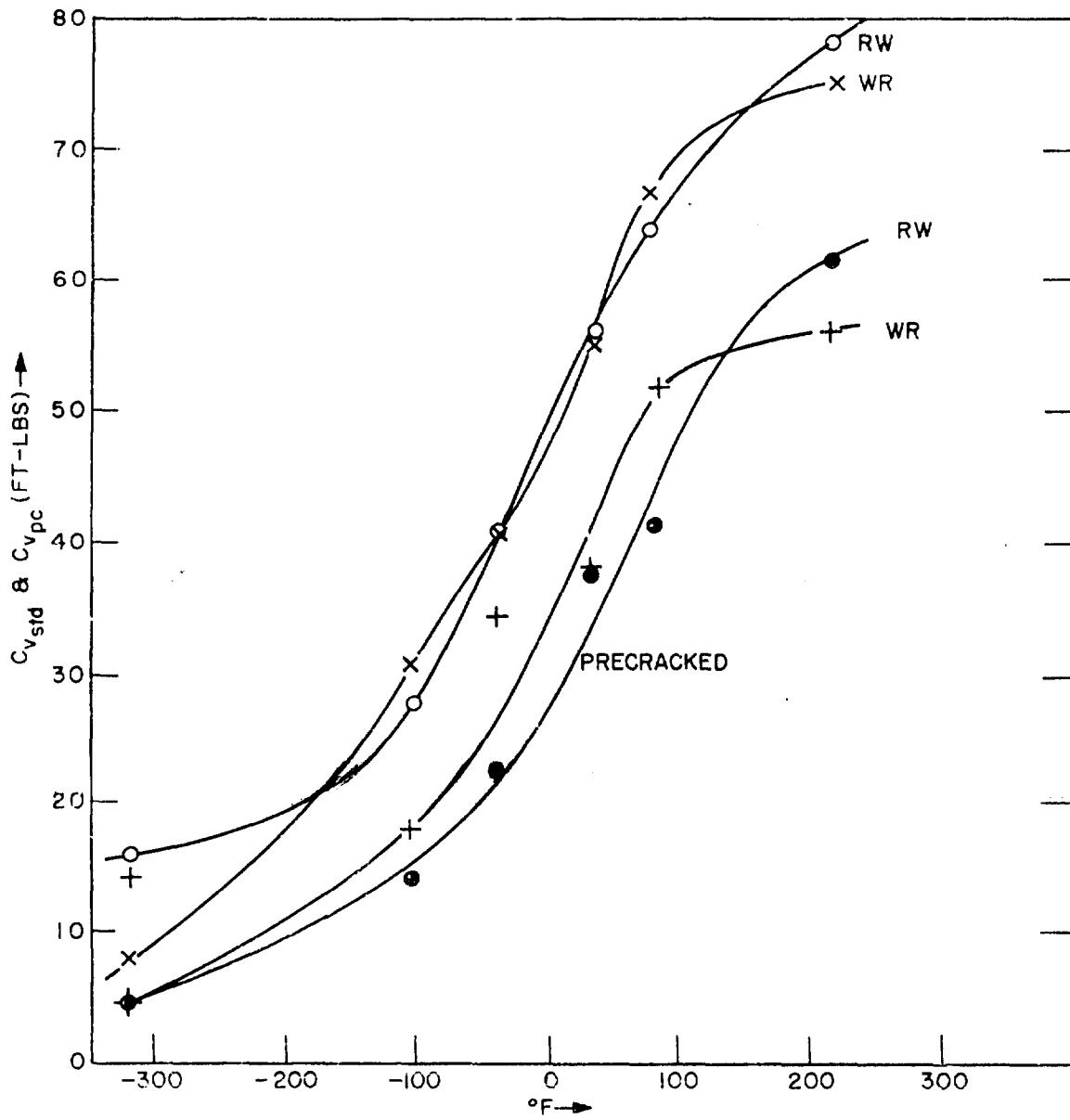
Fig. 27 - Standard and pre-crack Charpy V-notch properties of plate T-22 (Ti-6Al-2Mo) heat-treated at 1800°F for 1 hour in vacuum.
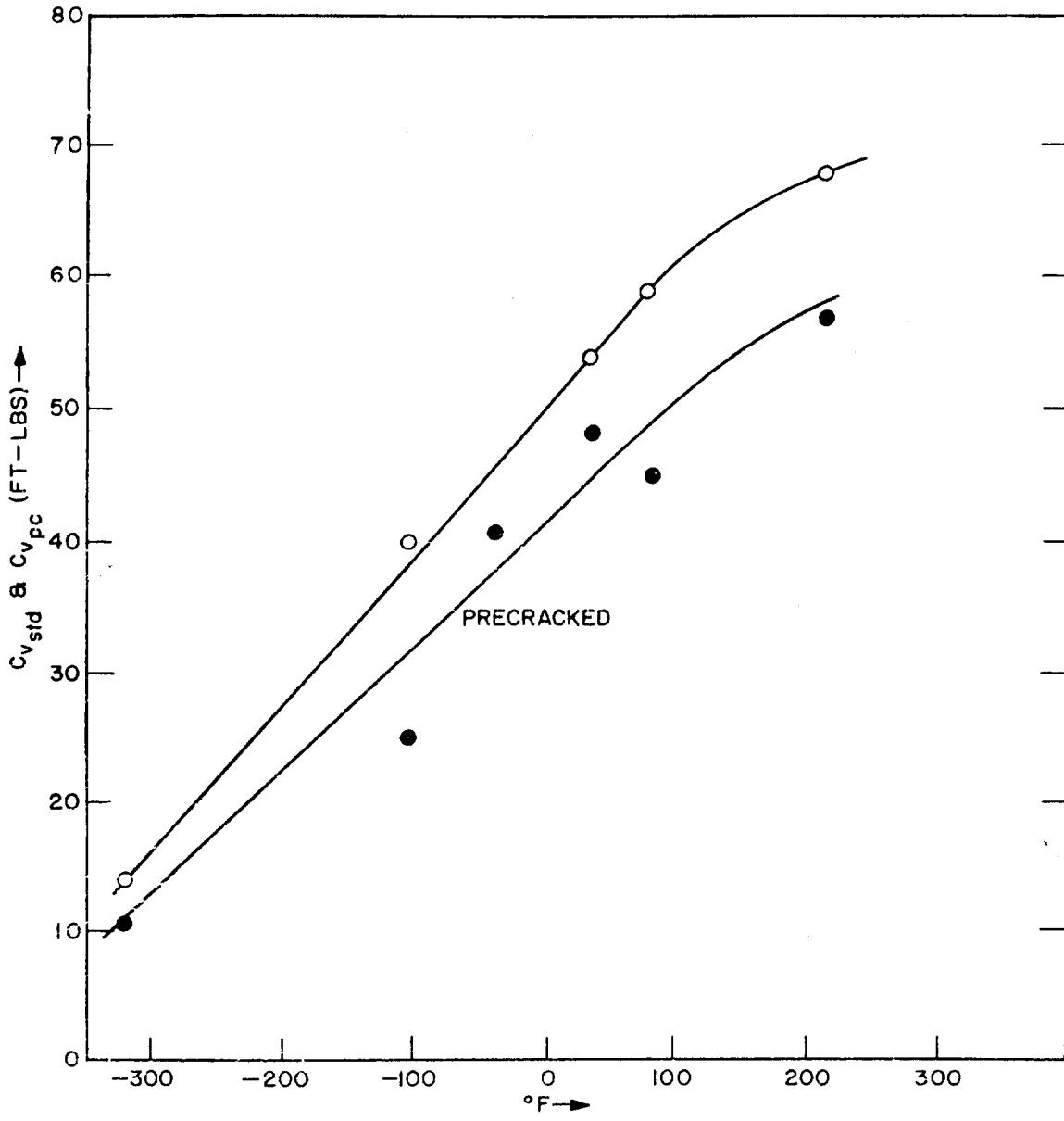
Fig. 28 - Standard and pre-crack Charpy V-notch properties of as-cast plate T-26 (Ti-7Al-2Cb-1Ta).
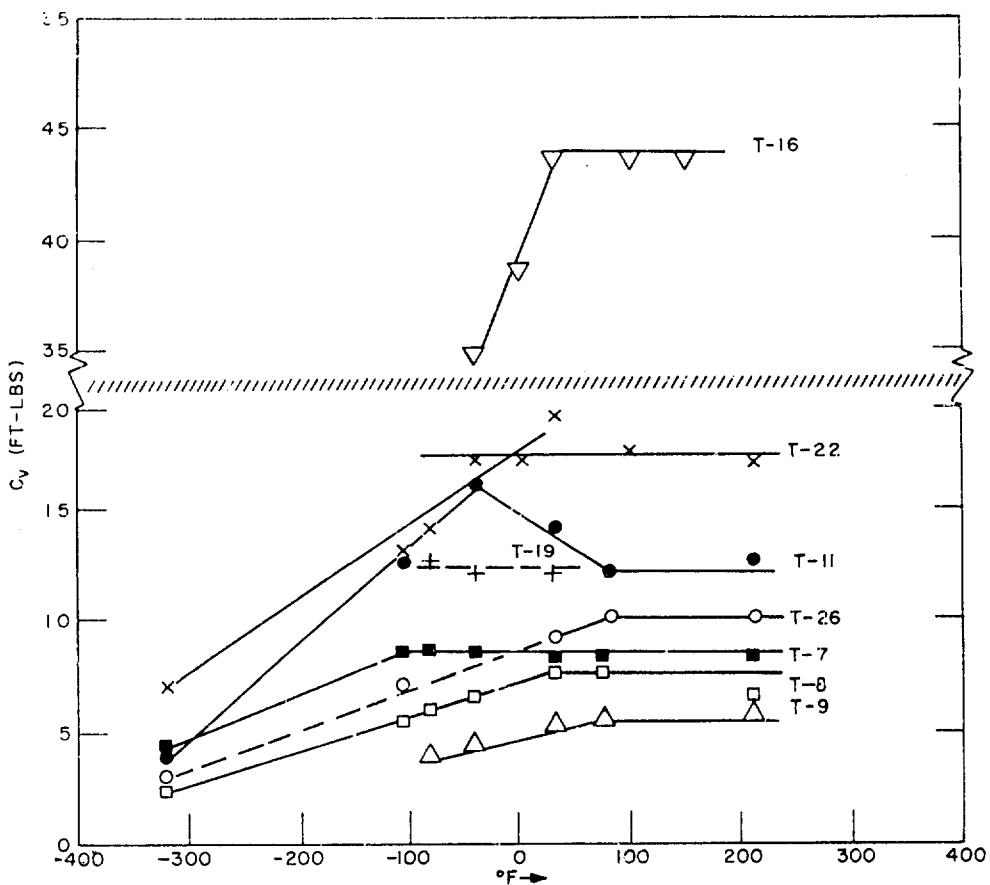
Fig. 29 - Relationship of energy required for fracture
initiation in standard Charpy V-notch specimens with
temperature for various titanium alloys.
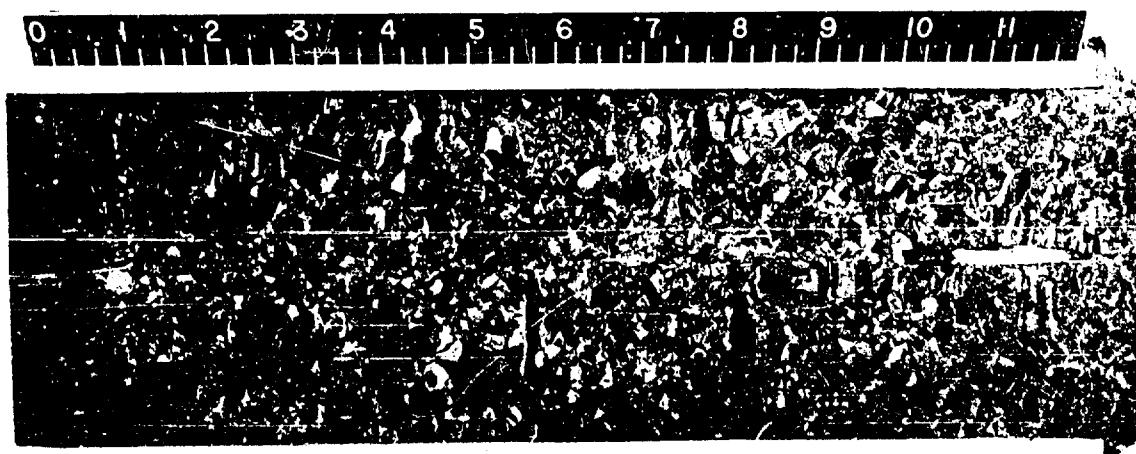
Fig. 30 - Photomacrograph of double arc-melted billet of
Ti-7Al-2Cb-1Ta extra low interstitial alloy, showing large
grain structure. Mag. 0.7x.
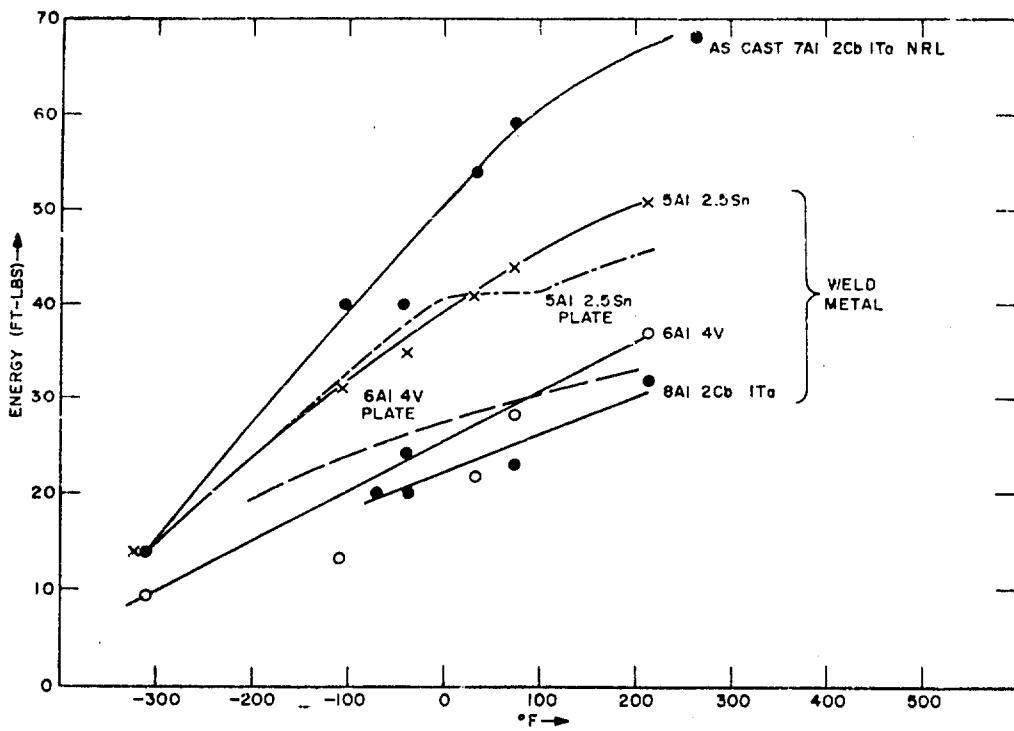
Fig. 31 - Charpy V-notch energy absorption
for titanium alloys.
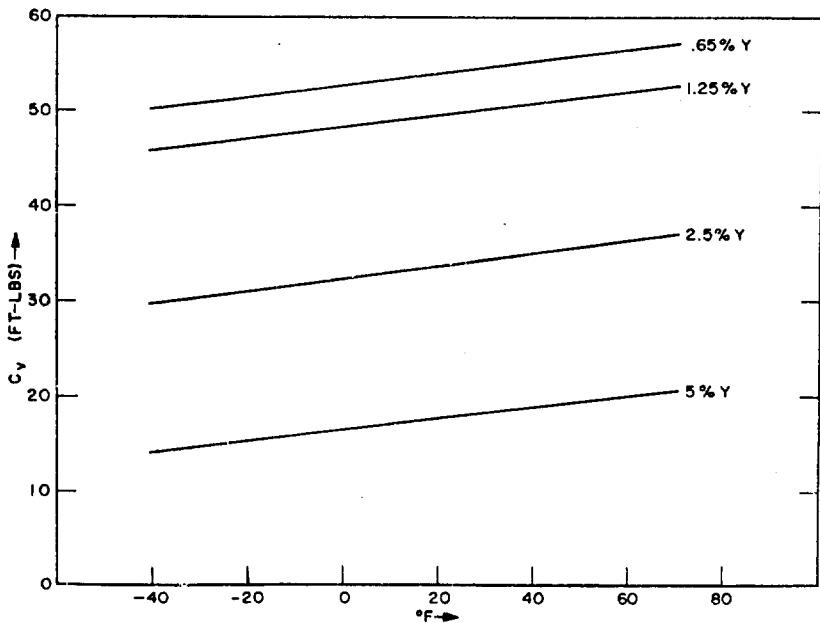
Fig. 32 - Nominal Charpy V-notch energy
absorption for titanium-yttrium alloys.